



Immunomodulation of Macrophages in Periapical Wound Healing

Citation

Andrada, Ana C. 2016. Immunomodulation of Macrophages in Periapical Wound Healing. Doctoral dissertation, Harvard School of Dental Medicine.

Permanent link

<http://nrs.harvard.edu/urn-3:HUL.InstRepos:33797368>

Terms of Use

This article was downloaded from Harvard University's DASH repository, and is made available under the terms and conditions applicable to Other Posted Material, as set forth at <http://nrs.harvard.edu/urn-3:HUL.InstRepos:dash.current.terms-of-use#LAA>

Share Your Story

The Harvard community has made this article openly available.
Please share how this access benefits you. [Submit a story](#).

[Accessibility](#)



**Immunomodulation of
Macrophages in Periapical
Wound Healing**



A Thesis presented by:

Ana Cristina Andrada, DDS

To

The Faculty of Medicine

In Partial Fulfillment of the Requirements

For the Degree of

Doctor of Medical Sciences

Research Mentor: Hajime Sasaki, DDS, PhD

The Forsyth Institute

Harvard School of Dental Medicine

April, 2016

Dedication

In loving memory of my father whose character and honesty were the best examples in my life.

To my mom, who has always supported and encouraged me to pursue my dreams. You provided me with a unique, loving, and cheerful childhood, which made it possible to be the person I am today.

To my best friend and husband, Luciano, and my son, Gustavo, for their unconditional love and support. You always encouraged me, believed in me, and pushed me forward even when I thought I could not go any further.

You made it all worth it!

Acknowledgement

I would like to express my sincere gratitude to my advisor and mentor, Dr. Hajime Sasaki for introducing me to the wonders and frustrations of scientific research. His guidance, encouragement, and support were fundamental for the development and completion of this research project.

I would like to thank my colleagues at the Forsyth Institute for their support at all times, especially Kimito and Shuang for their patience and willingness to help. I feel very fortunate to have had the privilege to work with you. My appreciation to my old friends and to the new ones I have met along the way for listening and holding my hand every time I needed some comfort.

I am grateful to my thesis proposal committee Dr. Susan Rittling, Dr. Toshi Kawai, and Dr. Xiaozhe Han for their advice and suggestions. Their extraordinary knowledge and relevant recommendations were crucial for the improvement of this study.

My greatest gratitude goes to my program director Dr. Robert White and Mrs. Linda White for their unlimited support inside and outside of the school. Their guidance, love, and care were essential during these stressful moments.

I would like to express my heartfelt thanks to my family for their endless love, support, and encouragement throughout my life and studies. You have believed in me and even from far away you were always there for me.

Thank you God for guiding me and molding me into who I have become.

Table of Contents

Abstract	9
Introduction	12
Review of Literature	14
1. Endodontic infections and periapical lesions	14
2. Macrophage Polarization	16
3. Selective M1/M2 Macrophage Depletion	19
a) Gadolinium Chloride	19
b) Mannosylated Clodronate Liposome	20
4. Azithromycin	21
5. Wound Healing	23
Specific Aims	25
Material and Methods	27
A. In vivo:	
1. Animals.....	27
2. Endodontic Pathogens	27
3. Induction of Periapical Lesion	28
4. Macrophage Depletion (preliminary study)	29
5. Antibiotic Treatment	29
6. Sample Isolation	30
7. Micro-computed Tomography Imaging (uCT)	31

8. Histological Analysis	31
9. mRNA Extraction from Bone Block	32
10. Quantitative Real Time Polymerase Chain Reaction (RT-PCR).....	35
 B. <i>In vitro</i> :	
1. Macrophage Polarization	36
a) Preparation of Mouse Blood Samples	36
b) Primary peritoneal macrophage isolation	36
c) Primary peritoneal macrophage cell culture for FACs analysis ...	37
d) Preparation of cells for flow cytometer (FACs) analysis	38
2. Stimulation of peritoneal macrophages for Elisa assay	38
3. Nitric Oxide production by peritoneal macrophages	39
4. NF- κ B(nuclear factor kappa B) reporter assay	39
Statistical Analysis	40
Results	41
1. The effect of Proposed Treatment on M1 and M2 Macrophages(FACS) 41	
a) Gadolinium Chloride (GdCl ₃)	42
b) Mannosylated Clodronate Liposome (MCL)	42
c) Azithromycin (AZM) vs. Ampicillin (AMP)	45
2. The effect of Azithromycin on the extent of mouse periapical lesions ...	48
a) Micro CT (uCT) analysis	49
b) Histological Analysis	54
c) Gene Expression Analysis	62
3. NF- κ B reporter Assay	73

4. Cytokine Expression of Stimulated Peritoneal Macrophages	75
5. Nitric Oxide Production by Stimulated Peritoneal Macrophages	77
Discussion	78
Conclusions	86
References	87

Tables and Figures

Table 1: Gene selection for RT-PCR	34
Table 2: Gene expression level of day 21 treatment groups	63
Table 3: List of genes on PBS group fold change > 2	64
Table 4: List of gene expression showing relevant fold change in AZM group	66
Table 5: List of gene expression showing relevant fold change in AMP group	68
Table 6: Gene expression level of AZM and AMP	70
Figure 1: Flow cytometry analysis on macrophage polarization	44
Figure 2: Flow cytometry analysis on M1 macrophage polarization <i>in vitro</i>	46
Figure 3: Flow cytometer analysis of M2 macrophage polarization <i>in vitro</i>	47
Figure 4: Representative uCT image of non-exposed and non-infected mouse mandibular first molar with normal periradicular tissues	49
Figure 5: Representative μ CT images of periapical lesions in Day 10 and PBS groups	50
Figure 6: Representative μ CT images of periapical lesions in the azithromycin and ampicillin experimental groups	51
Figure 7: Extent of periapical lesion in mm ²	52
Figure 8: Quantification of bone loss in the periapical region (mm ²)	53
Figure 9: Representative images of histological sections of Day 10	57
Figure 10: Representative images of histological sections of PBS group	58
Figure 11: Representative images of histological sections of Azithromycin group	59
Figure 12: Representative images of histological sections of Ampicillin group	60
Figure 13: Representative immunohistochemistry of anti-mouse Osteocalcin in mice periradicular tissue	61
Figure 14: PBS gene expression data arranged in a 3D profile	65
Figure 15: AZM gene expression data arranged in a 3D profile	67
Figure 16: AMP gene expression data arranged in a 3D profile	69
Figure 17: 3D profile of gene expression of AZM and AMP treated mice compared to day 21 PBS control	71
Figure 18: RANKL expression in periapical lesions	72
Figure 19: Luciferase activity with AZM stimulation	74
Figure 20: Cytokine expression in response to antibiotics	76
Figure 21: iNOS expression in response to antibiotics	77

Abstract

Background: A periapical lesion is an infection-induced inflammation around the apex of the tooth caused by bacterial invasion and ultimately results in the destruction of bone in the area. To date, the relationship between pathogens and the host immune system in the development of periapical lesions have been extensively investigated. However, a detailed understanding of the host factors that determine successful periapical wound healing is currently lacking. The long-term goal of the present study is to identify the molecular network that regulates wound healing and tissue regeneration in dentoalveolar infections in order to develop rational therapeutic approaches. Although a rodent model of periapical lesion was well established in Forsyth, adequate models for periapical wound healing are currently unavailable. Since the nature of apical periodontitis is infection-induced inflammation, the aim of this study was to systematically examine the effect of azithromycin treatment compared to ampicillin as a wound-healing treatment approach in mouse periapical lesions. Azithromycin is a macrolide antibiotic that specifically accumulates in macrophages exhibiting an anti-inflammatory effect via alteration of macrophage phenotype from pro-inflammatory M1 to anti-inflammatory M2 macrophages.

Material and Methods: Dental pulps of mandibular first molars in C57BL/6J mice (6 weeks of age) were surgically exposed and inoculated with a cocktail of common human endodontic pathogens, which are sensitive to employed antibiotics. Mice received daily doses of azithromycin (8 mg/kg), ampicillin (20 mg/kg) or phosphate-buffered saline (PBS) from day 10 to 20 post infection. No root canal treatments were provided.

Mandibles were isolated on days 10 (disease baseline) and 21. Right hemi mandibles were subjected to micro-computed tomography (μ CT) to determine the extent of periapical bone loss and subsequent histological and immunohistochemistry analysis. Left hemi mandibles were used for RNA extraction for gene expression analysis through quantitative RT-PCR. Moreover, primary peritoneal macrophages stimulated with LPS and treated with either azithromycin or ampicillin were evaluated for pro-inflammatory cytokines expression (using ELISA) and nitric oxide production (iNOS assay). The effect of azithromycin in the level of NF- κ B gene expression was assessed through luciferase reporter assay using Luciferase Stable RAW 264.7 cells.

Results: The μ CT results indicated that azithromycin treatment suppressed the extent of periapical bone loss compared to PBS treatment with a significant difference ($p < 0.05$) in the average size of periapical lesions. In addition, the extent of bone loss on Day 21 in azithromycin group was significantly “recovered” compared with the baseline disease group ($p < 0.05$). In histological observations, azithromycin-treated animals showed less neutrophil infiltration and a polarization of M2 macrophages in periapical lesions, while PBS treatment resulted in moderate neutrophil infiltration and an M1/M2-mixed macrophage profile. mRNA expression of pro-inflammatory cytokine IL-6 and chemokine CXCL2, as well as colony stimulating factor 2 (CSF2) had a significant down regulation in the azithromycin group when compared to baseline disease ($p < 0.05$). Up regulation of IL-4-mRNA was also observed. *In vitro* experiments confirmed the down regulation of IL-1 α and IL-1 β ($p > 0.05$) and nitric oxide production ($p < 0.05$) in LPS

stimulated peritoneal macrophages treated with azithromycin. Finally, the luciferase activity was decreased when cells were stimulated with azithromycin 50uM.

Conclusions: These results taken together suggest that the suppression of periapical bone loss by azithromycin appears to be dependent on its immunomodulatory properties. This report is the first finding on pro-resolving M2 macrophage polarization during periapical wound healing. This research can shed light to the development of a mouse model of periapical wound healing. In addition, this dual role of azithromycin, microbicidal and anti-inflammatory effects, could pose as a great adjuvant on the root canal therapy being highly translational.

Introduction

Endodontic infection is the infection of the root canal system and is the primary etiologic agent for periradicular inflammatory diseases (1, 2). A healthy root canal system is by nature an aseptic environment (3). The pathological process starts when the dental pulp becomes necrotic, either by caries, trauma or iatrogenic clinical procedures, and then infected by microorganisms that are usually inhabitants of the normal oral cavity flora (4). The environmental conditions in the necrotic root canal allow microbial colonization and multiplication, mainly by obligate anaerobic bacteria (5, 6). It is well established that the microorganisms and their by-products play a critical role on the development of pulpal and periradicular pathosis and their harmful effects have been the object of many studies over the years (1, 7). The host immune response to the root canal infection activates both innate and adaptive immune systems resulting in inflammation of periapical tissues and consequent bone destruction in the area known as apical periodontitis (8).

Macrophages are cells of the innate immune system which main role is to eliminate invading bacteria by phagocytosis and modulate adaptive immune responses by antigen presentation (9). Recent studies have shown the existence of different macrophage phenotypes, allowing us to better understand the properties and function of these cells. Diversity and plasticity are distinct features of macrophages (10). The early stages of the inflammatory process are typically associated with the M1 (pro-inflammatory) macrophages, which will induce inflammation and tissue damage known as acute inflammation. The M2 (anti-inflammatory) subtype predominates during the subsequent resolution removing cell debris and promoting tissue remodeling.

Azithromycin is a macrolide antibiotic shown to have immunomodulatory effects by accumulating in macrophages and shifting their polarization from a M1 to M2 phenotype (11).

In the present research, we explored the effect of azithromycin in the healing of mouse periapical lesion by testing the hypothesis that failure of macrophage activation and polarization into M2 (anti-inflammatory) macrophage results in chronic inflammation and persistent apical periodontitis.

Review of Literature

1. Endodontic infections and periapical lesions

A healthy root canal system is by nature an aseptic environment (3). Hence, upon exposure to microorganisms (usually inhabitants of the oral cavity) (4) due to caries, trauma or iatrogenic clinical procedures a pathological process starts leading to pulp necrosis. According to the American Association of Endodontists, more than 15 million root canal treatments are performed yearly in the US due to primary and secondary endodontic infections. Endodontic infection and necrotic pulp decrease the success and survival of endodontic therapy when compared to treatment of the inflamed dental pulp (12, 13). Even though endodontic outcome studies present great variability regarding the parameters used to assess success rates, like wide range of follow up, there is a consensus of opinion that presence of preoperative periapical lesion decreases the success rate of root canal treatment in about 10-15% (14, 15). In addition, patient presenting systemic diseases, like diabetes mellitus, have an even greater decrease in the success rate (16). Given the increasing prevalence of obesity and type 2 diabetes in the U.S. (>25 million and 8.3% of U.S. adults in 2011, respectively) (17), studies to elucidate the pathogenic mechanisms mediated by host factors in oral inflammation are essential so negative sequela in the endodontic treatment can be avoided in the future. Endodontic infections can cause signs and symptoms that range from mild discomfort to severe life threatening infections leading to serious systemic involvement such as cellulitis and angina (18, 19). There are profound consequences for patients and for the health care system due to the morbidity and cost of the management of non-healed cases. About 56% of all non-

traumatic dental emergencies are in the form of periapical abscesses and toothaches (20, 21). Finally, despite advances in the armamentarium for root canal treatment, like rotary files, ultrasonic irrigation and use of operating microscope, success have remained unchanged.

The microbial etiology of endodontic infections is well established (1, 2, 7) and its polymicrobial nature has been clearly demonstrated (1, 3). Once the root canal system has been contaminated, the microorganisms and their by-products play a critical role on the development of pulpal and periradicular pathosis.

A periapical lesion is an infection-induced inflammation view as an active confront between microbial factors and host defenses at the interface between infected radicular pulp and periodontal ligament. This encounter causes pathological changes at the tooth periapex in the form of tissue destruction and accumulation of inflammatory cells (8). Inflammatory mediators such as cytokines and chemokines are released in the area thus recruiting immune cells to participate in periapical defense (22). Cells of both the innate (neutrophils and monocyte/macrophages) and adaptive immune system (T cells, B cells and plasma cells,) play a role in the complex host response (23). The initial activation of the host response occurs through bacterial stimulation of toll-like receptors (TLRs) and nucleotide-binding oligomerization domain (NOD) receptors, both highly expressed in cells associated with periapical lesion including macrophages (24). As demonstrated by Hou *et al*, TLR4 deficient mice have reduced bone loss in the periapical area following endodontic infection due to decreased expression of inflammatory cytokines (25). Many studies have shown the presence of immunocompetent cells, such as T cells, plasma cells and macrophages in the periapical lesion (26, 27) and Stern *et al*

and Kawashima *et al* validated the predominance of macrophages in the area (28, 29). Periapical inflammatory infiltrates increase osteoclast numbers, and bone resorption is evident resulting in no reparative bone formation without treatment (30). Rapid bone destruction in the periradicular area can be attributed to proinflammatory cytokines such as IL-1 β , IL-1 α , receptor activator of nuclear factor kappa-B ligand (RANKL), TNF- α , IL-6 and IL-11 (23, 31).

A chronic infection develops as the necrotic tissue of the dental pulp is inaccessible to leukocytes and, therefore, represents a protected reservoir of bacteria (32). At this point, the host immune system is not fully competent to eliminate the invading pathogens and its by-products and a state of chronic inflammation is maintained. Modulation of the immune response is crucial for the achievement of complete wound healing in periapical lesion. The understanding of the role of M1 and M2 macrophages on those lesions and the development of new macrophage-centered therapeutic approaches is essential for the improvement of predictable periapical healing.

2. Macrophage Polarization

Macrophages are important effector immune cells found in all tissues derived from the maturation of blood circulating monocytes. They were first described by Ilya Metchnikoff (33) in 1892 and remain to be a topic of intense research until today. Macrophages exert crucial functions in non-specific or innate immune system, which include phagocytosis of invading microbes and ingestion of host apoptotic cells. Additionally, they act as antigen presenting cells to activate adaptive immune responses (34). Routinely, macrophages serve as surveillance phagocytic entities responsible for the

removal of senescent cells and cellular debris involved in physiological activities. This role is described as homeostatic clearance and happens independently of other immune cells (35). Moreover, they will sense danger signals thru pattern recognition receptors (PRRs) and rapidly respond to microbial invasion and tissue damage (36).

Toll-like receptors (TLRs) and NOD-like receptors (NLRs) are important pattern recognition receptors found on macrophages which function is to recognize the conserved molecular configurations of microorganisms known as pathogen-associate molecular patterns (PAMPs) (37). This interaction is characterized by an inflammatory response where reaction oxygen species (ROS) and cytokines are produced. The powerful pro-inflammatory reaction should be enough to contain the infection, however it can result in excessive tissue damage in some instances (36). Recruited monocytes have the ability to specialize into distinct tissue macrophages phenotypes in response to micro environmental stimulation. (38). This well-known characteristic so-called plasticity has long been recognized and is responsible for both pro and anti-inflammatory macrophage properties (39, 40). The macrophages will react differently to diverse stimulus and as a consequence, their activation response will give rise to different population of activated macrophages recognized as M1 or M2 (41).

The classically activated (M1) macrophages are activated in response to the cytokine interferon γ (IFN γ) alone or in conjunction with tumor-necrosis factor (TNF) or microbial products like lipopolysaccharide (LPS) (42). This activation mediates host defense against bacteria, viruses and protozoa and are also involved in antitumor immunity (35, 43). Natural killer (NK) cells of the innate immune system initially produce IFN γ priming macrophages to secrete pro-inflammatory cytokines and release

oxygen and nitrogen radicals to enhance their phagocytic ability. To sustain the macrophage activation, T helper 1 (Th1) cells will subsequently produced IFN γ providing a stable host defense (14, 20). M1 macrophages are characterized by their great capacity to produce interleukin-12 (IL-12) and interleukin-23 (IL-23) as well as CXCL9 and CXCL10 chemokines (44), being referred as IL-12^{high} and IL-10^{low}(42). Furthermore, they exert a bacteriostatic effect with the shift in iron homeostasis by repressing ferroportin and inducing H ferritin favoring iron sequestration (22, 23).

Another population of activated macrophages has been elucidated and called alternatively activated or wound healing (M2) macrophages. IL-4 and/or IL-13, immune complexes and toll-like receptor, IL-1 receptor ligands or IL-10 can induce this polarization (45). These macrophage phenotypes possess a distinct function being primarily involved in the resolution of the acute phase of inflammation and tissue remodeling as well as with parasitic diseases. M2 macrophages are characterized by a limited production of pro-inflammatory cytokines and high secretion of anti-inflammatory cytokines like IL-10, CCL18 and CCL22 and therefore described as IL-10^{high} and IL-12^{low}. Abundant levels of mannose receptor CD206 and scavenging receptor CD163 also characterize them (20, 21, 24).

An additional key aspect of macrophage polarization is the predominant arginine metabolism pathway in the ongoing immune response. The immune cell arginine metabolism is essentially involved in cancer, inflammation, infections, fibrotic diseases, pregnancy, and immune regulation in general. M1 macrophages carry the enzyme nitric oxide synthase (iNOS), which converts arginine to nitric oxide (NO) and citrulline known as the microbicidal and inflammatory pathway. NO can be further converted into reactive

nitrogen species that are fundamental defense against invading pathogens (46, 47). On the other hand, M2 macrophages express the enzyme arginase that transforms arginine to ornithine and urea. Ornithine is then converted into proline and polyamine, which favors proliferation as they are directly involved in collagen synthesis and cell proliferation respectively (47, 48).

It is fundamental to remember that M1/M2 polarization is a dynamic process and cells once polarized to pro-inflammatory phenotype can later be polarized to anti-inflammatory phenotype and vice versa. These changes are fast and appear at the levels of gene expression, protein, metabolite, and microbicidal activity in response to changes in the cytokine environment as demonstrated by Davis *et al* (49). Evidence is clear regarding the potential damage caused by macrophages on the host tissue. Following exposure to toxicants, the number of activated macrophages is increased resulting in dysregulated release of pro and/or anti inflammatory mediators that, respectively, exacerbate acute tissue injury or promote the progress of chronic diseases such as fibrosis and cancer (50). Experimental models have shown that some agents, such gadolinium chloride and mannosylated clodronate liposomes, could block macrophages and prevent tissue injury.

3. Selective M1/ M2 Macrophage depletion

1. Gadolinium Chloride

Gadolinium chloride (GdCl₃) is a rare earth metal shown to have the ability to block phagocytosis as verified by Roland *et al* in liver macrophages (Kupffer cells) (51). GdCl₃ can be considered a macrophage toxicant, and is used to inhibit the mononuclear

phagocytic system (52). It has been demonstrated that gadolinium completely blocks stretch-activated cation channels (53), voltage-gated Ca^{2+} channels (54) and voltage-gated Na^{+} and K^{+} channels. Due to Gd^{3+} ions and Ca^{2+} ions similarities it is believed that the biochemical effects induced by GdCl_3 occur through interference with intracellular calcium-dependent processes and calcium entry into cells (55). According to Miron *et al*, administration of gadolinium chloride (GdCl_3) *in vivo* is able to selectively deplete M1 macrophages. The inflammatory macrophages will phagocytose the GdCl_3 inducing their apoptosis via competitive inhibition of calcium and damage to plasma membranes. The same group also confirmed the selective depletion of M1 cells *in vitro* and was able to show that GdCl_3 did not affect the M2 cell number (56). Similarly, Pendino *et al* used GdCl_3 to suppress macrophage function and found that alveolar macrophages produced decreased quantities of nitric oxide and $\text{TNF-}\alpha$, and expressed less inducible nitric oxide synthase (iNOS) (57).

2. Mannosylated Clodronate Liposomes

Mannosylated clodronate liposomes (MCLs) can be used for selective depletion of M2 macrophages. Once liposomes are phagocytized by macrophages their phospholipid bilayers are disrupted by lysosomal phospholipases and clodronate is released intracellularly. Clodronate cannot cross the cell membrane and accumulates in the cell. At a certain intracellular concentration, irreversible damage causes the macrophage to be killed (58). Miron *et al* was able to selectively deplete M2 macrophages *in vivo* and *in vitro* with administration of MCLs. They bind the mannose

receptor that is highly express in M2 macrophages, inducing apoptosis within 2-3 days via clodronate-mediated depletion of intracellular iron (56).

4. Azithromycin

Azithromycin (AZM) is a semi-synthetic macrolide antibiotic, which presents broad-spectrum antibacterial activity (11). Macrolide antibiotics are drugs with a macrocyclic lactone ring containing from 12 to 16 atoms to which are attached one or more sugars (59). Erythromycin A was the first macrolide clinically used, being isolated in the early 1950s from cultures of *Streptomyces* (60). Macrolides reversibly bind to the 23S rRNA and consequently, inhibit protein synthesis (61). Likewise, azithromycin inhibits bacterial protein synthesis by binding to 50S ribosomal subunit and interfering with elongation of peptide chain (62). AZM is effective against aerobic and anaerobic gram-negative and gram-positive bacteria, blocks quorum-sensing and inhibit formation of biofilm (63). It has been widely used for a great variety of infections, including upper and lower respiratory tract infections, and has been shown to have beneficial effects in chronic inflammatory disorders. The efficacy in these conditions has been attributed to immunomodulatory effects on innate and adaptive immune responses (11). Azithromycin has a large volume of distribution, high tissue concentration, extended half-life and is efficiently delivered to sites of infection (64). As reported by Lode *et al*, AZM half-life is approximately 70h (oral formulation) or 50h (intravenous), allowing infrequent dosing and greater patient compliance (65).

Azithromycin presents a very remarkable feature that is the accumulation into phagocytic cells. AZM is taken up by those cells, delivered to sites of inflammation and

then released during the process of phagocytosis to deliver locally high concentration of the drug (65). Due to this characteristic, AZM concentration in tissue have been reported to be up to 100 fold higher than in plasma (66) in several body tissues including periodontal pockets (67). The immunomodulatory effects of azithromycin include but are not limited to, down regulation in production of neutrophil chemokines (IL-8, CXCL1, MPO) (68). Moreover, a decrease in production of tumor necrosis factor- α (TNF- α) and granulocyte-macrophage colony stimulating factor (GM-CSF) in LPS-stimulated human macrophages has been reported (69). Additionally, AZM has been shown to shift the polarization of activated (M1) macrophages towards the alternative/ anti-inflammatory (M2) phenotype.

Several studies have reported the role of azithromycin on the polarization of macrophages to a M2 phenotype. Murphy *et al* investigated the *in vitro* effect of the drug in mouse macrophage cell line (J774) and concluded that AZM altered the macrophage phenotype. The authors have shown a decrease in production of pro-inflammatory cytokines and expression of M1 markers. On the other hand, M2 cell markers (mannose receptor and CD23) and anti-inflammatory cytokines were up regulated (70). Furthermore, they have confirmed the same finds in a murine model of lung infection (71). Another research group (72) also demonstrated an increase in expression of mannose receptor in alveolar macrophages from chronic obstructive pulmonary disease (COPD) patients *in vitro*. Reduced brain infiltration of inflammatory cells (neutrophils and macrophages) and induction of M2 polarization by AZM contributed to neuroprotection against ischemic stroke injury in mice (73).

We believe that macrophage polarization towards anti-inflammatory/ pro-fibrotic (M2) phenotype is crucial for the wound healing of periapical lesions. To date, there are no reports correlating the use of azithromycin and macrophage polarization in the periradicular tissues. This lack of evidence and gap in knowledge provided inspiration and was fundamental for the elaboration of this study.

5. Wound Healing

It is essential that we understand the wound healing of periapical lesions. The process starts as soon as the chemomechanical cleaning and shaping of the root canal system is achieved. It is well known that inflammation is an essential part of the normal wound healing process, aiding on the clearance of invading microorganisms and restoring tissue homeostasis (74). Early stages of wound healing are characterized by abundant production of pro inflammatory cytokines by innate immune cells, with the objective of create an environment that protects the host from microbial infection (74). The process starts with the recruitment of neutrophils and macrophages to try to contain the infection. Later, the adaptive immune system is activated and cytokines and chemokines will promote macrophage shifting from M1 to M2 phenotype, the so-called late stage of wound healing. In the late stages, macrophages undergo a phenotypic transition to a reparative stage, promoting clearance of the apoptotic cells, angiogenesis and tissue remodeling. These cells are said to be responsible for the switch from the inflammatory to the proliferative stages of wound healing (35, 74, 75). When the root canal is effectively disinfected, the macrophage shifting occurs and wound healing takes place.

Optimum wound healing and factors affecting the process is well discussed in cutaneous wounds, however, a detailed understanding of the host factors that determine successful periapical wound healing is currently lacking. Our long-term goal is to identify the molecular network that regulates wound healing and tissue regeneration in dentoalveolar infections in order to develop rational therapeutic approaches.

Specific Aim

The goal of the present study is to shed light on the understanding of endogenous regulatory mechanisms of inflammation and wound healing in periapical lesions. A rodent model of periapical lesion is well established, however a gap in knowledge remains regarding a rodent model of periapical wound healing after the establishment of periradicular infection. Evidence to date indicates that the shift of the phenotypic behavior of pro-inflammatory (M1) to anti-inflammatory (M2) macrophages is beneficial to modulate disease and promote tissue remodeling (76). Several drugs have been shown to promote this polarization, including azithromycin (56, 70). Besides its anti-microbial behavior, azithromycin shows anti-inflammatory properties. These properties combined make AZM a good approach for macrophage polarization in mice. Our rationale is that mice treated with azithromycin will have an increased pro-resolving M2 macrophage polarization and improved periapical wound healing.

Hypothesis

We hypothesized that stimulation of M2 macrophage polarization will promote wound healing and induction of bone formation in mouse periapical lesions.

We will test our hypothesis by pursuing the following Specific Aims:

Specific Aim 1: To identify the best approach for M1/M2 polarization. Gadolinium chloride (GdCl₃) and mannosylated clodronate liposomes (MCLs) will be employed to deplete M1 and M2 macrophages respectively. Azithromycin will be used to look at the effect of macrophage polarization.

Specific Aim 2: To determine the best treatment approach for M2 macrophage activation in periapical lesion. Azithromycin, Ampicillin and PBS treated mice will be compared to baseline diseased animals regarding the effect of treatment on the size of developed periapical lesions. M1/M2 macrophage profile will be analyzed by histology and immunohistochemistry.

Material and Methods

1. In vivo:

1. Animals:

Male and female C57BL/6J wild type (WT) mice of 6 weeks of age were purchased from The Jackson Laboratory (Bar Harbor, Maine, USA). The animals were maintained in a specific pathogen free (SPF) environment at The Forsyth Institute Animal Facility, housed in cages with filtered air circulation where the temperature was kept at 70 +/- 5 degrees Fahrenheit with 50 +/- 20% relative humidity in accordance with the guidelines of the Institutional Animal Care and Use Committee. A 12-hour light/dark cycle was maintained and the animals were fed standard rodent chow and water at libitum. The Forsyth Institute Institutional Animal Care and Use Committee (IACUC) approved all experimental protocols before initiation of any experiment.

2. Endodontic Pathogens:

Four common endodontic pathogens including *Prevotella intermedia* (ATCC 25611), *Streptococcus intermedius* (ATCC 27335), *Fusobacterium nucleatum* (ATCC 25586), and *Peptostreptococcus micros* (ATCC 33270) were selected as representatives of human endodontic microbiota not endogenous to mice (77). The pathogens were grown on 15 x 100 mm blood agar plates (5% Sheep Blood in Tryptic Soy Agar (TSA) Base; Hardy Diagnostics) under anaerobic conditions (85% N₂, 10% H₂, and 5% CO₂) for 48 hours. The cells were harvested and suspended in prerduced anaerobically sterilized Ringer's solution (PRAS) (Anaerobe system-Morgan Hill, CA). The final concentration of each organism was determined spectrophotometrically, and the four

species of microorganism were mixed to yield a concentration of 10^{10} cells of each species/ml, resulting in a total of 4×10^{10} in 2% of methylcellulose (Parchem Methylcellulose, A4M Food Grade) (31).

3. Induction of Periapical Lesion:

Periapical lesions were induced in both mesial and distal roots of mandibular first molars by surgical pulp exposure with exception of non-exposed/non-infected negative control mice: n=20 for preliminary study (macrophage depletion) and n=55 for azithromycin study. Mice were anesthetized with 62.5 mg/kg ketamine HCl and 12.5 mg/kg xylazine in sterile phosphate-buffered saline (PBS) by intraperitoneal (I.P.) injection, using 26G needles (5/8 inch). Animals were placed on a jaw retractor board and right and left mandibular first molar pulps were exposed using a sterile dental round bur size $\frac{1}{4}$ (SS White) mounted in a variable speed electric handpiece (Endo DTC® Endodontic Motor; Aseptico, Woodinville, WA) under a surgical microscope (model MC-M92; Seiler, St. Louis, MO). The exposure site was typically equivalent to 1.5-fold the diameter of the bur. The pulp chamber was opened until the entrances of both mesial and distal canals could be visualized with the help of a microsurgical mirror (Hu-Friedy, Chicago, IL) and probed with a #6 endodontic file (Dentsply). At the time of pulp exposure (day 0), animals were infected with 10 μ l of the bacterial mixture inoculated directly into the exposed pulp by a 26 gauge needle. An endodontic file #6 was used to deliver the bacterial suspension into the mesial and distal root canals. The animals were monitored until recovering consciousness and placed back in their equivalent cages. Exposed pulps were left open during the 21 days of experimental protocol.

4. Macrophage Depletion (preliminary study):

On Day -1 relative to dental pulp exposure, mice received i.p. injection of either PBS or gadolinium chloride (GdCl₃); or intravenous injection (retro orbital) of control blank liposome or mannosylated clodronate liposome (MCL). GdCl₃ was used for selective depletion of pro-inflammatory M1 macrophages while MCL was used to selectively deplete anti-inflammatory M2 macrophages.

Filtered GdCl₃ (Santa Cruz Biotechnology, Dallas, TX) in PBS (2.5 mg/mL; 100 μ l = 0.25 mg per mouse) was used for the injections. Sterile PBS was used as vehicle control. Since re-population of deleted cells starts from Day 3 post injection (55), GdCl₃ treatments were conducted on Days -1, 2, 5, 8, 11, 14, and 17 relative to pulpal exposure.

M2 macrophage depletion kit, consisting of MCL and control blank liposome was purchased from Encapsula Nano Sciences. 100 μ l of m-Clodrosome[®] (Mannosylated Liposomal Clodronate) was used for each injection. The dose of clodronate disodium salt is 5 mg/mL, and 100 μ l = 0.5 mg. 100 μ l of m-Encapsome control liposomes was used as control (Mannosylated Clodrosome Kit). Intravenous injections (retro orbital vein plexus) were performed. MCL treatments were conducted on Days -1, 6, and 13 relative to pulpal infection according to a previous study conducting long-term macrophage depletion (78).

5. Antibiotic treatment:

Azithromycin (500mg/vial) and ampicillin (1gram/vial) for injection were purchased from the Henry Schein animal health, Dublin, Ohio. On day 10 after pulp exposure, mice were randomly divided in 4 groups: 1) Disease baseline (Day 10 post exposure); n=10; 2) Ampicillin-treated; n=15; 3) Azithromycin-treated; n=15; and 4)

PBS-injected (vehicle/positive control); n=15. Daily injections of Ampicillin, Azithromycin and PBS were performed from day 10 to day 20 on the remaining groups. The route of injection was intraperitoneal (i.p.), and 26G needles (5/8 inch) were used. Treatment regimen was performed as follows: 0.2 mg azithromycin in 200 uL PBS/mouse/day was given once a day for initial two days, then the dose was reduced to 0.1 mg/day in remainder of 8 days (based on 500 mg (initial dose/adult (60 kg)/day for pneumonia); 0.2 mg ampicillin in 200 uL PBS/mouse, once a day from day 10 to 20 relative to the pulp exposure (based on 1000 mg/adult (60 kg)/day for such as urethritis); PBS (200uL) was injected as a vehicle control from day 10 to day 20 post pulp exposure.

Animals were sacrificed on Days 0 (non-infected control), Day 10 (Disease baseline) and Day 21 (experimental groups and positive control group) after the pulpal infection by carbon dioxide (CO₂) asphyxiation following Forsyth standard operating procedure. Decapitation was conducted for sample isolation.

6. Sample Isolation:

After death mice were decapitated, mandibles were isolated and hemi-sectioned. Right hemi mandibles were fixed in fresh 4% paraformaldehyde in PBS for at least 24 hours and submitted to uCT analysis and subsequent histological analysis. Left hemi mandibles were immediately placed in liquid nitrogen and frozen at -80 degrees Celsius until RNA extraction.

7. Micro-computed tomography imaging (uCT):

The right hemi mandibles fixed in paraformaldehyde of all C57BL/6J wild type (WT) mice used in the study (experimental and control) were analyzed at Forsyth Institute by a compact fan-beam-type tomograph (μ CT40 system, Scanco Medical AG, Bassersdorf, Switzerland) (79). The specimens were washed in PBS and placed in a cylindrical sample holder filled with distilled water. The samples were positioned in Styrofoam and aligned in the same manner in each tube for consistency. For each sample, approximately 300 micro-tomographic slices with an increment of 10 μ m were acquired, covering the entire width of the mandible. Each sample took about 1 hour for the complete scanning. Data sets in DICOM format were re-sliced and analyzed using the Image J software (Wayne Rasband, National Institute of Health, Bethesda, MD). Pivotal sections including the crown and distal root of the mandibular first molar exhibiting a clear access opening and patent root canal apex were selected for quantitation. The periapical lesion size was measured using Adobe Photoshop CS6 (Adobe Systems, San Jose, CA). The area including the bone loss around the distal root of maxillary first molar was expressed as square millimeters (mm^2) using a standardized template.

8. Histological Analysis:

Fixed hemimandible samples used for mCT analysis were decalcified using 10% EDTA, dehydrated in ethanol, replaced with xylene and finally embedded in paraffin. Following serial sectioning at 6 μ m thickness, every fifth specimen was mounted and stained with H&E following standard histological procedure. Following initial observation, sections containing the region of interest (patent root canal with localized

periapical lesion) were selected, mounted, and subjected to immunohistochemistry using the avidin-biotin peroxidase method for identification. Briefly, after deparaffinization using xylene and graded ethanol series, each section was subjected to endogenous peroxidase inhibitory treatment by 0.3% hydrogen peroxide with methanol (both Sigma-Aldrich) for 30 minutes and protein blocking treatment used Protein Block (DAKO) for 10 minutes. We employed the following 6 antibodies: 1) anti-mouse Mac2 antibody (total macrophage; 1:500, BioLegend); 2) anti-mouse Ly6G antibody (neutrophil; 1:1000, BioLegend); 3) anti-mouse iNOS antibody (M1 macrophage; 1:500, Abcam), 4) anti-mouse Arg-1 antibody (M2 macrophage; 1:500, Abcam); 5) anti-mouse Osteocalcin (osteoblast; 1:500, Abcam); and 6) anti-mouse Cathepsin K (osteoclast; 1:500, Abcam). Antigen-antibody complexes were evidenced by the avidin-biotin peroxidase (ABC) method, using a commercially available kit DAB Peroxidase (HRP) Substrate Kit (DAKO). Finally, the sections were counterstained with hematoxylin, dehydrated in graded alcohol series, cleared in xylene and cover slipped with Eukitt (Sigma-Aldrich). The specificity of immune reactions was tested by omission of primary antibodies and/or substitution with isotype control. Cell enumeration and distribution analyses were carried out under light microscopy either at x100, x200 or x400 magnification.

9. mRNA Extraction from Bone Block:

The left hemi mandibles were removed from -80°C, had their ends trimmed, transfer to an eppendorf tube containing 500 microliter (µl) of pre chilled RNAlater®-ICE (Ambion® life technologies) and kept overnight in -20°C to inactivate RNase. On the next morning, soft tissues including gingiva, oral mucosa, muscles, and ligaments

were defleshed under a surgical microscope and tooth crown was dissected free of the samples and discarded. A bone block containing the periapical tissues surrounding the mesial and distal root apices of the mandibular first molar was carefully extracted and transfer to a Lysing Matrix A tubes (MP Biomedical) containing 2 ceramic spheres. 1 milliliter (ml) of TRIzol® Reagent (Ambion® life technologies) was added to the tube and the contents were immediately disrupted using a high-speed homogenizer FastPrep®-24 Instrument (MP Biomedical) for 20 seconds. Two cycles were performed. Subsequently, 200 microliter (µl) of chloroform was added to the tubes, incubated at room temperature for 3 minutes and centrifuged. The mixture was transferred to a Phase-lock gel tube (5-Prime) and centrifuged for 5 minutes for phase separation. The separated aqueous phase solution containing total RNA was carefully transferred to a new tube. Isopropanol 99.5% was added in a 1:1 ratio and after centrifugation, a pellet of RNA was visible. The separated RNA was washed twice with 70% ethanol and air dried for 5 minutes. RNA pellet was resuspended in 35 µl of RNase free water. RNA samples were then tested for purity and quantified using spectrophotometer Nanodrop 2000c (Thermo Scientific). Samples showing 260/280 ratios of 1.7-2.0 were used for further qRT-PCR analysis.

	Correspondence between gene name and bar in 3D figures	Gene	Forward Sequence 5'-3'	Reverse Sequence 5'-3'
Inflammatory response	A3	Cxcl2	TTC ATG GAA GTG TGC AT	ACA CGA AAA GGC ATG ACA AA
	A4	IL-10	AGT GGA GCA GGT GAA GAG TG	TTC GGA GAG AGG TAC AAA CG
	A5	IL-17a	TCC AGA AGG CCC TCA GAC TA	ACA CCC ACC AGC ATC TTC TC
	A6	IL-1a	CGG GTG ACA GTA TCA GCA	GAC AAA CTT CTG CCT GAC GA
	A7	IL-1b	CCC AAC TGG TAC ATC AGC AC	TCT GCT CAT TCA CGA AAA GG
	A8	IFN γ	TTA ACT CAA GTG GCA TAG	TGA TTC AAT GAC GCT TAT
	A9	Ccl5 (Rantes)	CCT CAC CAT CAT CCT CAC TG	TGA CAA ACA CGA CTG CAA GA
	A10	Ccr1	ACC GTA CCT GTA GCC CTC AT	GCC AGG TCC AGT TGC TTA CT
	A11	IL-1rn	TTC AAA GCC CTT TCT TGT TG	GAG TCA CTT GGG GCA TAT TG
	A12	IL-6	CTA CCC CAA TTT CCA ATG CT	ACC ACA GTG AGG AAT GTC CA
	B1	Ptgs2 (Cox2)	AGA AGG AAA TGG CTG CAG AA	GCT CGG CTT CCA GTA TTG AG
	B2	TNF	CTA TGT CTC AGC CTC TTC TC	CAG CCT TGT CCC TTG AAG AG
	B3	Ccl11 (Eotaxin)	GCT CTG AGG GAA TAT CAG CA	CCT AAC TCG TCC CAT TGT GT
	B4	Lta (TNF-b)	TGG TTC TCC ACA TGA CAC TG	ATG GGT CAA GTG CTT CTG AG
	B5	NFKB-1	TGA GAA TGG ACA GAA CAG CA	AAG CTG AAC AAA CAC GGA AG
	B6	Nos 2 (iNOS)	CTT TGT GCG AAG TGT CAG TG	CAC CTG GAA CAG CAC TCT CT
Inflammasome	D1	Aim2	ATA CAA AGG CAG TGG GAA CA	ATC TCA CAG TCC CAG GAT CA
	D2	Casp 1 (Ice)	TGG CAC ATT TCC AGG ACT GA	TCT TTC CAT AAC TTC TGG GCT TT
	D3	Nlrc4 (Ipadf)	CTT GGC CAG GAG AGC CTT GC	ACT TCC CTT TGC CAG ACT CG
	D4	Nlrp-1a	TCC TGG TGG CTG AAA AGT GA	TGC ATT CAT GGT GGG TCA GG
	D5	Nlrp3	GAC ACG AGT CCT GGT GAC TT	TAG ACT CCT TGG CGT CCT GA
	D6	Myd88	TGT TCT TGA ACC CTC GGA CG	CGA AAA GTT CCG GCG TTT GT
	D7	Ripk2	CCA TCC CGT ACC ACA AGC TC	GCA GGA TGC GGA ATC TCA AT
	D8	Casp 12	TGC TGG ATT GGC CCA TGA AT	GGG AAC CAG TCT TGC CTA CC
Osteogenesis	E1	Bmp2	TTG CAC ACT TGC TGT CTG TT	GTT CTC ACG GAT TGG ACA AC
	E2	Bmp3	GGT TGA GAG GAG GAA GAA GC	TTC TTC AGG GTC TGC TCA TC
		TNFs11	AAT TCC CCT GAA GGT ACT CG	TCC TTT TTG GCT ATG TCA GC
	E3	Bglap (osteocalcin)	AAG CAG GAG GGC AAT AAG GT	TGC CAG AGT TTG GCT TTA GG
	E4	Col1a1	ATG ATG CTA ACG TGG TTC GT	TGG TTA GGG TCG ATC CAG TA
	E5	Spp1 (osteopontin)	GAC CCA TCT CAG AAG CAG AA	TTC GTC AGA TTC ATC CGA GT
	E6	OPG	ACT GCA CAG TGA GGA GGA AG	TCA AGC AGA ATT CGA TCT CC
Wound healing	F1	IL-4	CAA GGT GCT TCG CAT ATT TT	ATC CAT TTG CAT GAT GCT CT
	F2	CSF-2(GM-CSF)	CAG GGT CTA CGG GGC AAT TT	ACA GTC CGT TTC CGG AGT TG
	F3	Fgf2	CGT TGT ACA CTC AAG GGG CT	GTC CCG TTT TGG ATC CGA GT
	F4	CSF-1	GAC CCT CGA GTC AAC AGA GC	TGT CAG TCT CTG CCT GGA TG
	F5	TGFb 1	GCT ACC ATG CCA ACT TCT GT	CGT AGT AGA CGA TGG GCA GT
Macrophages	C1	CD86	GCA AGG TCA CCC GAA ACC TA	TGT CAG CGT TAC TAT CCC GC
	C2	CD80	TTC ACC TGG GAA AAA CCC CC	CCC GAA GGT AAG GCT GTT GT

	C3	CD163	CAT GTC TCT GAG GCT GAC CA	TGC ACA CGA TCT ACC CAC AT
	C4	CD43	AGA GGC CAC AAC CAC ATC AG	AAG AAC GTA GTG AGC GTG GG
	C5	CCR2	GGG CTG TGA GGC TCA TCT TT	TGC ATG GCC TGG TCT AAG TG
	C6	CX3CR1	GTG ACA TGA AGA GGG ACC TG	CCC TCG CTT GTG TAG TGA GT
	C7	Ly6C	CTTGCTCTGATGGTCCTCC	ACTTACCCAGCAGGGGCTAT
House Keeping	A1	GAPDH	CTGGAGAAACCTGCCAAGTA	TGTTGCTGTAGCCGTATTCA

Table 1. Gene selection for RT-PCR

10. Quantitative Real Time Polymerase Chain Reaction (RT-PCR):

The synthesis of complimentary DNA (cDNA) was performed using iScript™ cDNA Synthesis Kit (Bio-Rad Laboratories) by adding 1 ug of purified total RNA, 4ul of 5x iScript reaction mix and 1ul of reverse transcriptase in a total of 15ul solution. Quantitative Real Time Polymerase Chain Reaction (RT-PCR) was performed using Kapa Sybr® Fast qPCR Kit Optimized for LightCycler® 480 in a LightCycler® 480 System (Roche). Pre-incubation cycle of 3 min at 95°C was performed. The temperatures and times for denaturation, annealing, and elongation were 95°C for 10 seconds, 58°C for 20 seconds, and 72°C for 1 second, respectively, which were repeated for 50 cycles. Melting curve analysis was also performed with a single cycle of 95°C for 5 seconds; 65°C for 60 seconds and 97°C prior to the final cooling at 40°C. The 2^{-ddCT} was used for data analyses. The expression level of each gene was normalized to the corresponding GAPDH expression level. Azithromycin, ampicillin and PBS (Day 21) groups were compared to baseline disease group (day 10). Table 1 shows the genes chosen for the experiment. Likewise, AZM and AMP groups were compared to PBS.

2. In vitro:

1. Macrophage Polarization

a) Preparation of Mouse Blood Samples:

Blood was drawn from the retro orbital vein plexus of one mouse of each treatment group from the preliminary study as previously described: 1) Gadolinium Chloride; 2) PBS; 3) Mannosylated Clodronate liposomes; 4) Blank liposomes. Approximately 500 microliters (μl) of blood was obtained from each mouse using heparinized pipettes. Blood was diluted in 2 milliliter (2ml) of PBS and slowly transferred to a new tube containing 3ml of histopaque[®] 1083 (Sigma, Saint Louis, Missouri). Tubes were centrifuged at 1500 rpm for 30 min at room temperature. Red blood cells separated from white blood cells (WBC) and were deposited in the bottom of the tube. WBCs remained in the plasma/histopaque interface and were carefully transfer to a new tube. Cells were washed with PBS and centrifuged at 400xg for 5 min. Washing steps were repeated to remove any remaining histopaque[®] 1083 from the mononuclear cells. Cells were fixed with 4% paraformaldehyde (PFA) in PBS and kept in 4°C.

b) Primary peritoneal macrophage isolation:

Non-infected C57BL/6J mice were euthanized in CO₂ chamber, sprayed with 70% ethanol and placed on the dissection table. The abdominal skin was dissected and 5ml of cold Roswell Park Memorial Institute 1640 (RPMI-Gibco) medium was injected into the peritoneal cavity using a 26-gauge needle. The abdominal cavity was massaged to dislodge the macrophages and the entire body was shaken for 10 seconds to mix the medium well. Medium containing the macrophages were slowly drawn with an 18-gauge

needle beveled side down. The needle was left in place and another 5ml of RPMI was injected and aspirated. The cells were centrifuged, the supernatant was discarded and cells resuspended in 1ml of fresh RPMI medium supplemented with 10% fetal bovine serum (FBS). Nine ml of medium was added and cells were once again centrifuged. The washing step was repeated and cells were ready to be counted. The cells were seeded as follows: for ELISA assays = 1×10^5 cells/ 100 μ l/ well in 96 well plate; and FACS assay = 3.5×10^6 cells/ 35mm plate.

c) Primary peritoneal macrophage cell culture for FACS analysis:

Peritoneal macrophages (3.5×10^6 cells/35 mm plate) were pre-cultured in a humidifier incubator at 37°C containing 5% humidified CO₂ for 6 hours to allow macrophages to adhere firmly to the dish. Experimental plates were pre-incubated for 1h with azithromycin or ampicillin and cells were stimulated as follows for 12 hours:

1. Control: medium only
2. LPS: for M1 activation (0.1ug/ml)
3. M-CSF: for M2 activation (10ng/ml)
4. LPS (0.1ug/ml) + Azithromycin (4ug/ml, 60uM)
5. LPS (0.1ug/ml) + Ampicillin (100ug/ml)

Cells were then harvested with 2.5mM EDTA in PBS, washed and fixed in 4% paraformaldehyde (PFA) in PBS and kept in 4°C.

d) Preparation of cells for flow cytometer (FACS) analysis:

Cells from mouse blood as well as cells from peritoneal macrophages were prepared for FACS analysis. Cells were added to FACS tubes in a concentration of $1 \times 10^6 / 100 \mu\text{l}$. $2 \mu\text{l}$ of Fc receptor blocking antibody (TruStain fcX™ (anti-mouse CD16/32), BioLegend) was added for 5min prior to immunostaining. The following antibody stains (BioLegend, San Diego, CA) were added to the cells: a) FITC anti-mouse CD68 for total macrophages; b) APC anti-mouse CD80 for M1 macrophages; c) PE/Cy7 anti-mouse CD206 for M2 macrophages. Unstained cells were used as control. Flow buffer consisting of 5% Fetal Bovine serum (FBS) plus 1mM EDTA in PBS was then added to each sample, shaken gently and centrifuged. Supernatant was collected, mix with fresh flow buffer and flow cytometry was performed using The BD FACSAria™ II cell sorter (BD Biosciences). Data were analyzed by FlowJo software (Tree Star, Ashland, OR).

2. Stimulation of peritoneal macrophages for ELISA assay:

Peritoneal macrophages (10^6 cells/ well in 96-well plate) were pre-cultured with azithromycin (30uM) and ampicillin (100ug/ml) for 2 hours and then washed with RPMI supplemented with 10% FBS to remove non-adherent cells such as lymphocytes. Adherent cells were considered as macrophages and were stimulated with LPS (0.1ug/ml) for 20 hours in presence/absence of azithromycin (30uM) and ampicillin (100ug/ml). Non-stimulated/non-treated cells served as negative control, and cells stimulated with LPS alone served as positive control. Culture supernatants were collected 20 hours after incubation and subjected to Elisa assay to determine the level of IL-1 α and IL-1 β using

commercially available cytokine ELISA kits (DuoSets, R&D systems). The assays were conducted following the manufacture's instructions. The concentration of each cytokine was calculated based on a standard curve constructed with specific recombinant cytokine provided in each kit. The results were measured in pg cytokine/ml of culture supernatant.

3. Nitric Oxide production by peritoneal macrophages:

Peritoneal macrophages were harvested as described above and seeded in a concentration of 3.0×10^5 cell/ well in a 48-well plate. Cells were pre-incubated with azithromycin (46ug/ml, 60uM) and ampicillin (100ug/ml) for 1 hour and then stimulated with lipopolysaccharide (LPS, 0.1ug/ml). Cells were cultured in a humidifier incubator at 37°C containing 5% humidified CO₂ for 12 hours. Cell supernatants were subjected to Nitrate/Nitrite Colorimetric Assay (Cayman Chemical, Ann Arbor, MI) to measure the production of nitric oxide (NO) by activated macrophages. The results were measured and calculated from a standard curve and NO production was expressed in uM.

4. NF-κB (nuclear factor kappa B) reporter assay:

The luciferase reporter assay is widely used as a tool to study gene expression at the transcriptional level. A commonly used reporter gene is the luciferase gene from the firefly *Photinus pyralis* (80). This gene encodes an enzyme that oxidizes D-luciferin, yielding a fluorescent product that can be quantified by a luminometer. To determine the level of NF-κB gene expression under proposed experimental conditions below, NF-κB Luciferase Stable RAW 264.7 cells (Applied Biological Materials, Canada) were employed. The cells were seeded in a 48-well plate (1.5×10^5 cell/ well), pre-incubated

with azithromycin in 3 different concentrations (12.5uM; 25uM and 50uM) for 1 hour and then stimulated with LPS (0.1ug/ml) for 12 hours. Medium alone was used as a baseline control and cells stimulated with LPS but no antibiotics served as positive control. The effect of antibiotics on LPS-stimulated luciferase activity was measured using Luciferase Assay System kit (Promega, Madison,WI) and absorbance read in Synergy HT (BioTek) reader.

Statistical Analysis

In analyses of numerical data sets, the effect of one factor (e.g. treatment effect) on more than three groups (e.g. the extent of periapical lesions) was determined using One-way Analysis of Variance (ANOVA) and corrected by Dunnett's Post Hoc test. Two-tailed Student's t-test was used to compare the effect of one factor between two groups. In either analysis, the p value less than 0.05 was considered as statistically significant.

Results:

Our proposed Specific Aim 1 was to identify the best approach for shifting of macrophage phenotype. The goal of this aim was to understand the feasibility of shifting the macrophage phenotype from the classically activated M1 macrophage to the alternatively activated M2 under either LPS or bacteria stimulation with the use of Gadolinium chloride (GdCl₃), mannosylated clodronate liposomes (MCLs) and azithromycin.

1. The effect of proposed treatments on M1 and M2 macrophages (FACS)

In order to evaluate selective depletion of each polarized macrophage population in mouse periapical lesions we chose to use Gadolinium (III) chloride (GdCl₃) and mannosylated clodronate liposome (MCL) as they are shown to selectively deplete pro-inflammatory (M1) and anti-inflammatory (M2) macrophages respectively (56). Pulp exposure was performed in both mandibular first molars and teeth were infected with endodontic pathogens. GdCl₃ experimental group (n=5) received intra peritoneal injections (2.5mg/ml; 100 ul/ mouse) on days -1, 2, 5, 8, 11, 14, and 17 relative to pulpal infection PBS group (n=5) served as vehicle control receiving injections on the same schedule (100 ul of sterile PBS). In MCL groups, intravenous injections (5mg/ml; 100 ul/mouse) of MCL experimental group (n=5) and blank liposome control group (n=5) were performed on days -1, 6, and 13 relative to pulpal infection. Blood samples were collected from all animals on day 21 and the population of M1 and M2 macrophage polarization was analyzed through flow cytometry.

a) Gadolinium (III) Chloride (GdCl₃):

According to previous reports gadolinium chloride can inhibit phagocytosis and reduce the number of M1 resident macrophages (81). Miron *et al* successfully demonstrated the ability of pro-inflammatory M1 macrophage depletion by GdCl₃ (56).

Although we expected a considerable decrease in M1 phenotype, our results showed (Fig.1: M1 depletion) that even though a decrease in M1 macrophage population could be observed in GdCl₃ treated group that was no difference between GdCl₃ and remaining experimental groups, including its PBS control group:

- The ratio of M2/M1 cells was 1.98 in PBS group while it was 2.01 in GdCl₃ group;
- GdCl₃ treatment increased population of both M1 and M2 macrophages (x1.2 and x1.23, respectively);

No difference in M1 depletion between the PBS and GdCl₃ groups suggesting that GdCl₃ is not the best approach for our research.

b) Mannosylated Clodronate Liposome (MCL):

Our expectation of selectively deplete M2 macrophages was founded on the reports from Miron *et al*. When M2 polarization occurs MCLs will bind to up regulated mannose receptor on those cells inducing apoptosis (56).

Selective depletion of M2 macrophages was effective in MCL treated mice in our experiment. MCL treatment increased the ratio of M1/M2 (1.74) compared to that in blank liposome (BL) group (0.76). In addition, MCL treatment reduced M2 population (0.7-fold vs BL) whereas M1 population was increased by the MCL treatment (4-fold vs

BL). Unexpectedly blank liposome consistently reduced both M1 and M2 population compared to PBS control, suggesting a possibility that BL suppresses immune response vs PBS treatment (Fig. 1: M2 depletion).

M1 Depletion

M2 Depletion

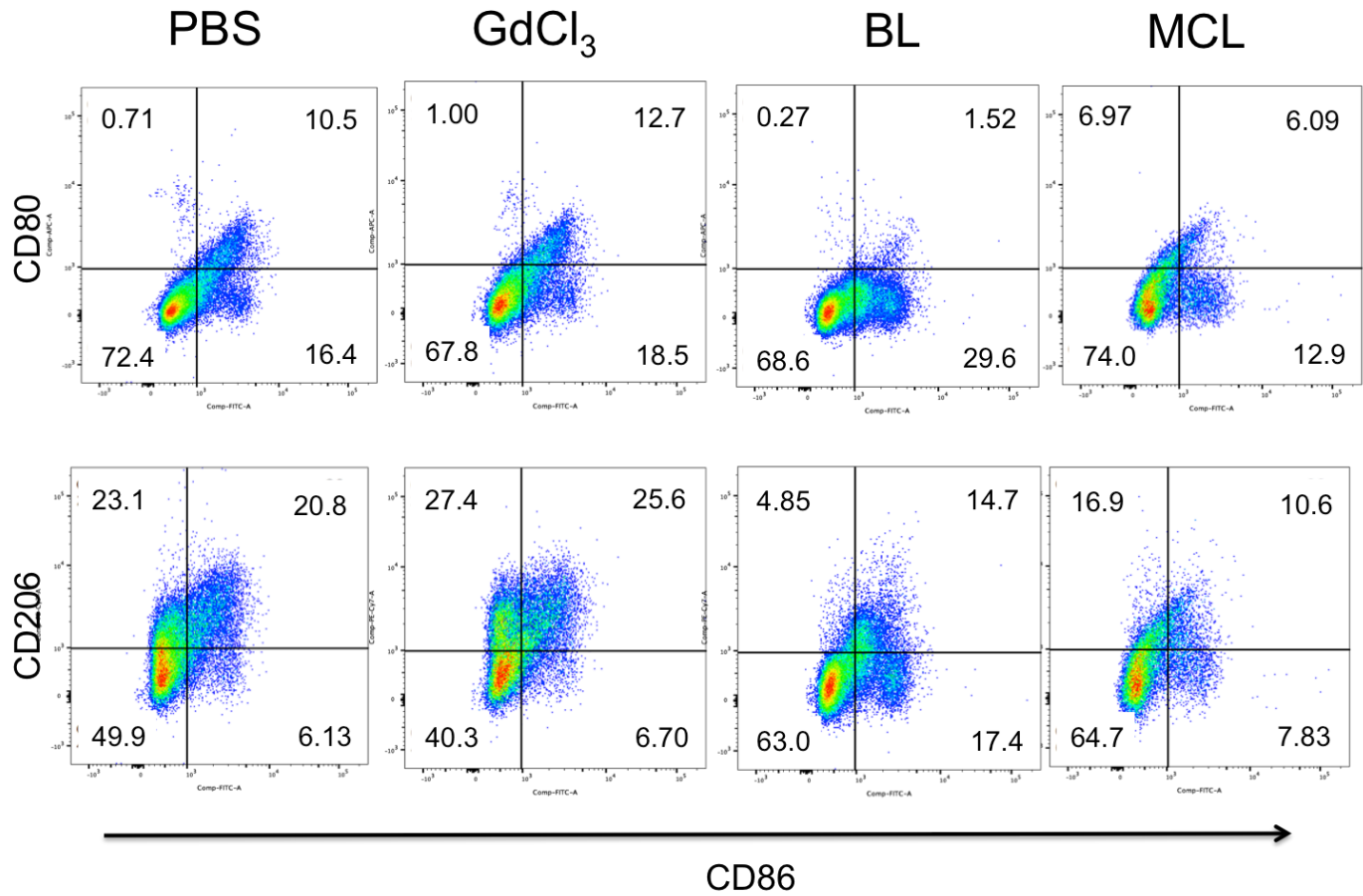


Figure 1. Flow cytometry analysis on macrophage polarization. Representative scatterplots of the 4 treatment groups showing M1 and M2 macrophage population. CD80 marker defines M1 cells represented on the top set of plots. CD 206 is used for M2 cells shown on the bottom set of plots. CD86 marker shown on the X-axis represents total macrophage population.

c) Azithromycin (AZM) vs. Ampicillin (AMP):

To compare the effect of azithromycin and ampicillin on the polarization of macrophages from a classical to an alternatively activated phenotype, we cultured primary peritoneal macrophages isolated from mice at 6 weeks of age. Cells were pre-incubated with either azithromycin or ampicillin for 1 hour and then stimulated with LPS for 12 hours in the presence of antibiotics in the same condition. To serve as M1 macrophages control, cells were stimulated with LPS alone. The cells stimulated with M-CSF served as M2 macrophages control. Non-stimulated cells served as a negative control. The cells were stained with specific macrophage markers and subsequently submitted to flow cytometry analysis.

The results obtained (Fig. 2) indicated that both azithromycin and ampicillin reduced the expression of M1 macrophages (CD80 marker) when compared with stimulation with LPS only. AMP suppressed M1 activation and the percentage of M1 macrophages was similar to the control group. In contrast, AZM reduced M1 population (even under LPS stimulation) similar to the M-CSF treated cells. When looking at the M2 marker (CD206) we noticed that azithromycin, but not ampicillin, up-regulated the expression of M2 macrophages. In AMP group, the M2 population was similar to LPS group, while in AZM group, M2 population was higher in comparison to LPS but lower than M-CSF group (Fig.3).

In a series of experiments, only AZM treatment exhibited consistent phenotypic shift of the macrophage population to M2 macrophages. Thus, I mainly used AZM in subsequent experiments.

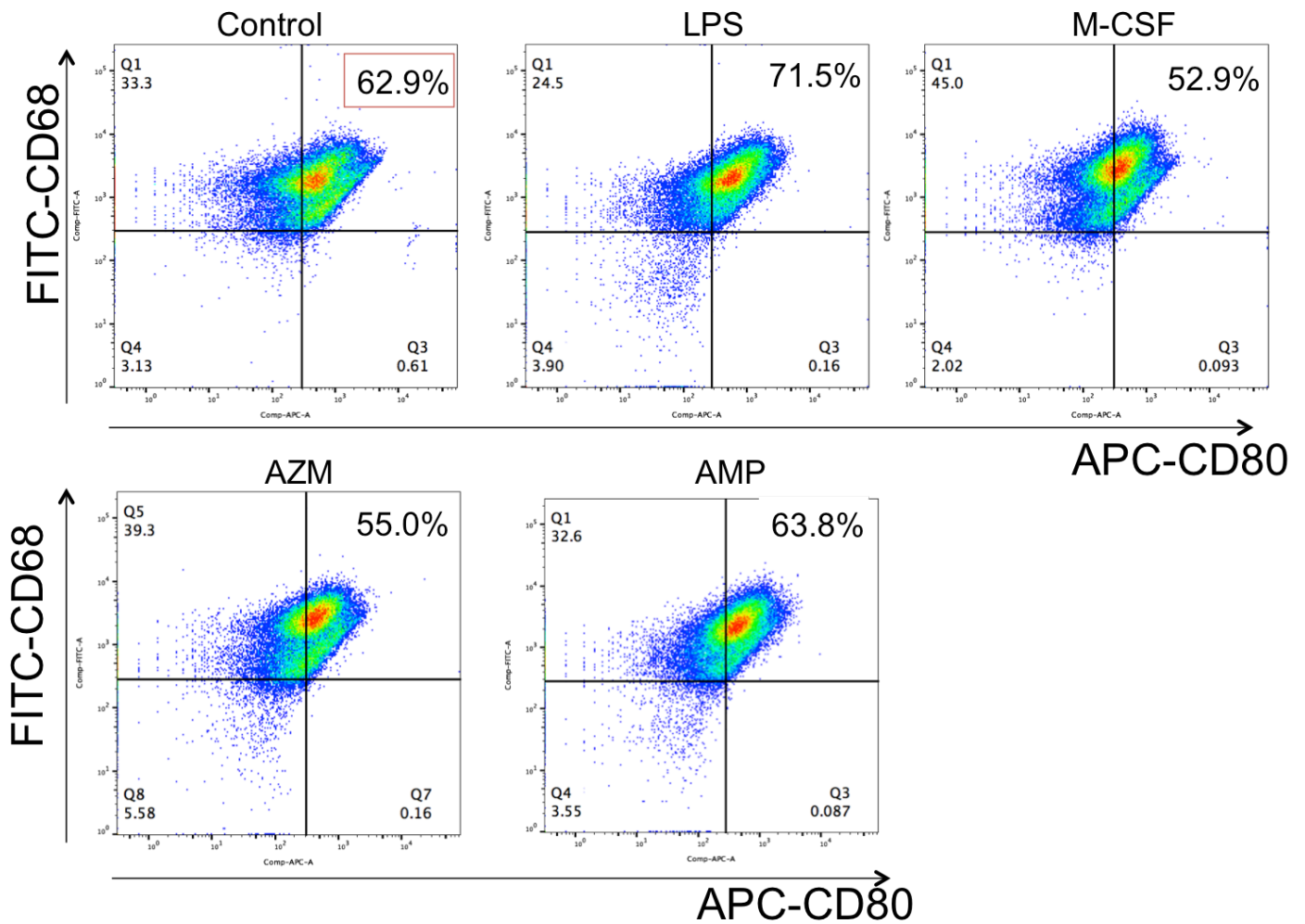


Figure 2: Flow cytometry analysis on M1 macrophage polarization *in vitro*:

Scatterplots of stimulated peritoneal macrophages. Y-axis represents total macrophage cells stained with FITC CD68 marker. X-axis shows cells stained with APC CD80 (M1) marker. AZM presents a strong suppression of M1 polarized macrophages comparing to the other stimulants.

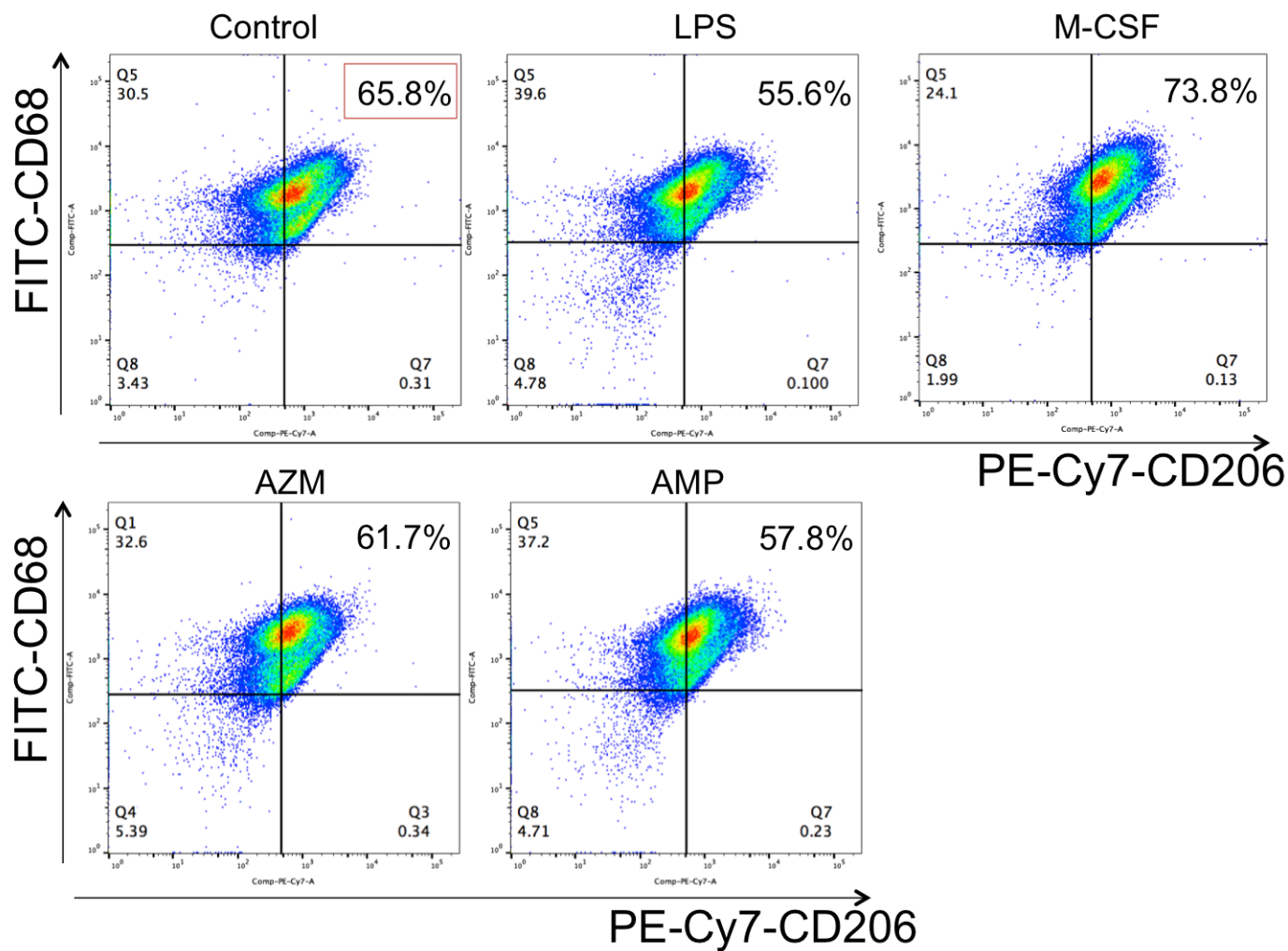


Figure 3: Flow cytometer analysis of M2 macrophage polarization *in vitro*: Plots showing FITC CD68 marker cells (total macrophages) on the Y-axis and PE-Cy7 CD206 (M2 macrophage) marker cells on the X-axis. Up-regulation of M2 marker can be seen on AZM stimulated group. AMP had no affect on the CD206 (M2) marker cell expression.

Ampicillin did not change macrophage population serving as a good control substance vs. azithromycin.

The Specific Aim 2 of this study predicts to determine the best treatment approach for M2 macrophages activation in periapical lesion. As described above, azithromycin was the treatment of choice for further experiments.

2. The Effect of Azithromycin on the Extent of mouse periapical lesions

Evidence to date indicates that azithromycin can shift the phenotypic behavior of classically activated macrophages (M1) to alternatively activated (M2) (70). AZM contains a distinctive immunomodulatory effect that combined with its broad spectrum antimicrobial properties make it a perfect drug of choice for various infections. The drug has been used for the treatment of chronic inflammatory disorders (11) and its anti-inflammatory property has been shown to improve lung function in cystic fibrosis patients (82, 83). The presence of macrophages in the periapical lesion is well established (81) but their role in the wound healing of those lesions still to be determined.

To assess the effect of azithromycin in the wound healing of mouse periapical lesions, we treated the animals with daily injections of AZM. Same scheduled of injection were given to ampicillin (AMP) and phosphate buffered saline (PBS) groups for comparison. Intra-peritoneal injections started 10 days after pulp exposure and root canal contamination with endodontic pathogens and were carried out until day 21 when mice were sacrificed.

a) Micro CT (uCT) Analysis

In order to measure the amount of periapical bone destruction, a non-invasive and rapid method was used (Fig. 4). Micro CT scanning was performed as described by Balto *et al* (79) on right hemi-mandibles of all groups (baseline disease, azithromycin, ampicillin and PBS). The distal root of the mandibular first molar was selected for the bone loss measurement. The periapical lesion size was measured in mm² using Adobe Photoshop CS5 (Fig. 5, 6 and 7).

As shown in (Fig. 5, 7) periapical bone destruction was induced after 10 days after pulp exposure. The extent of periapical lesion on day 10 was set as the disease baseline. On day 21, the PBS group (no treatment) had practically the same extent of bone resorption. Azithromycin treatment consistently suppressed the extent of periapical bone loss compared to PBS group with a significant difference ($p < 0.05$) in the average size of periapical lesions. In addition, the extent of bone loss on Day 21 in azithromycin group was significantly *recovered* compared with the baseline group ($p < 0.05$) suggesting that azithromycin is inducing bone formation on the area (Fig.6, 7).

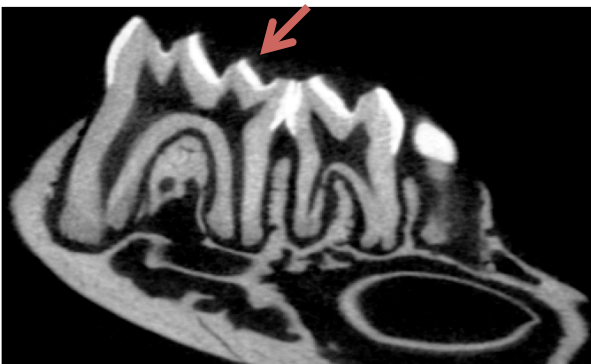


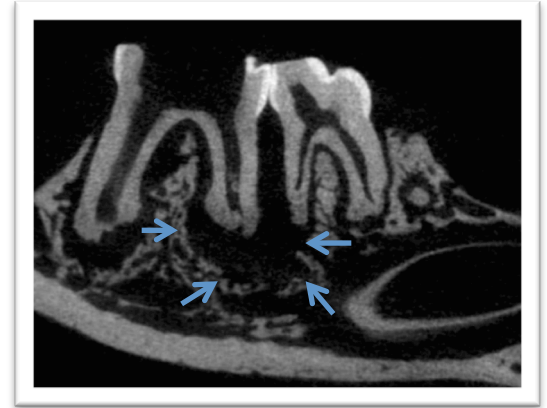
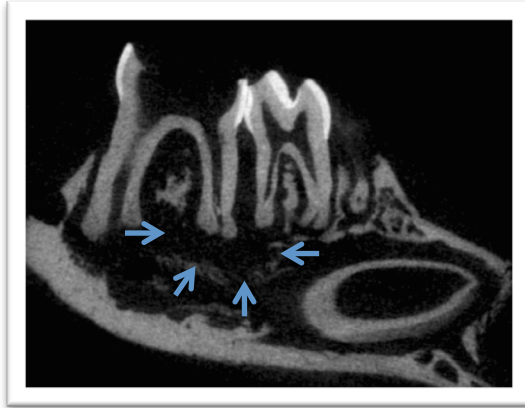
Figure 4: Representative uCT image of non-exposed and non-infected mouse mandibular first molar with normal periradicular tissues.

The lamina dura surrounding the distal root is intact and the periodontal ligament is uniform.

Day 10

PBS Day 21

A)



B)

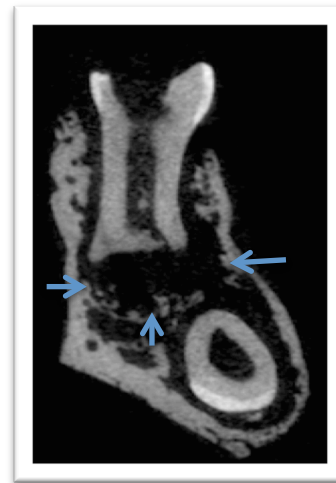
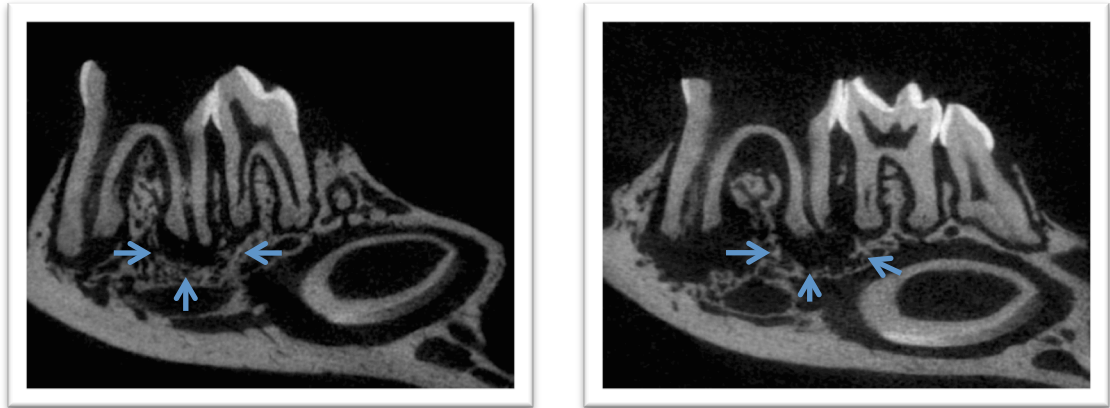


Figure 5: Representative μ CT images of periapical lesions in Day 10 (baseline disease) and PBS (day 21) groups. (A) buccal-lingual view; (B) proximal view of distal root. Arrows demarcate periapical lesion.

AZM Day 21

AMP Day 21

A)



B)

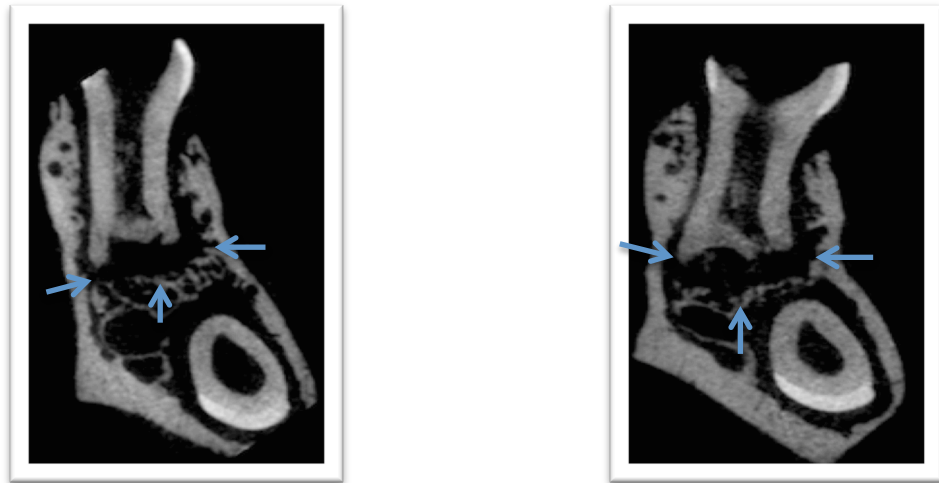


Figure 6: Representative μ CT images of periapical lesions in the azithromycin and ampicillin experimental groups. (A) buccal-lingual view; (B) proximal view of distal root. Arrows demarcate periapical lesion. Azithromycin treated animals presented decrease in lesion size compared to the other groups.

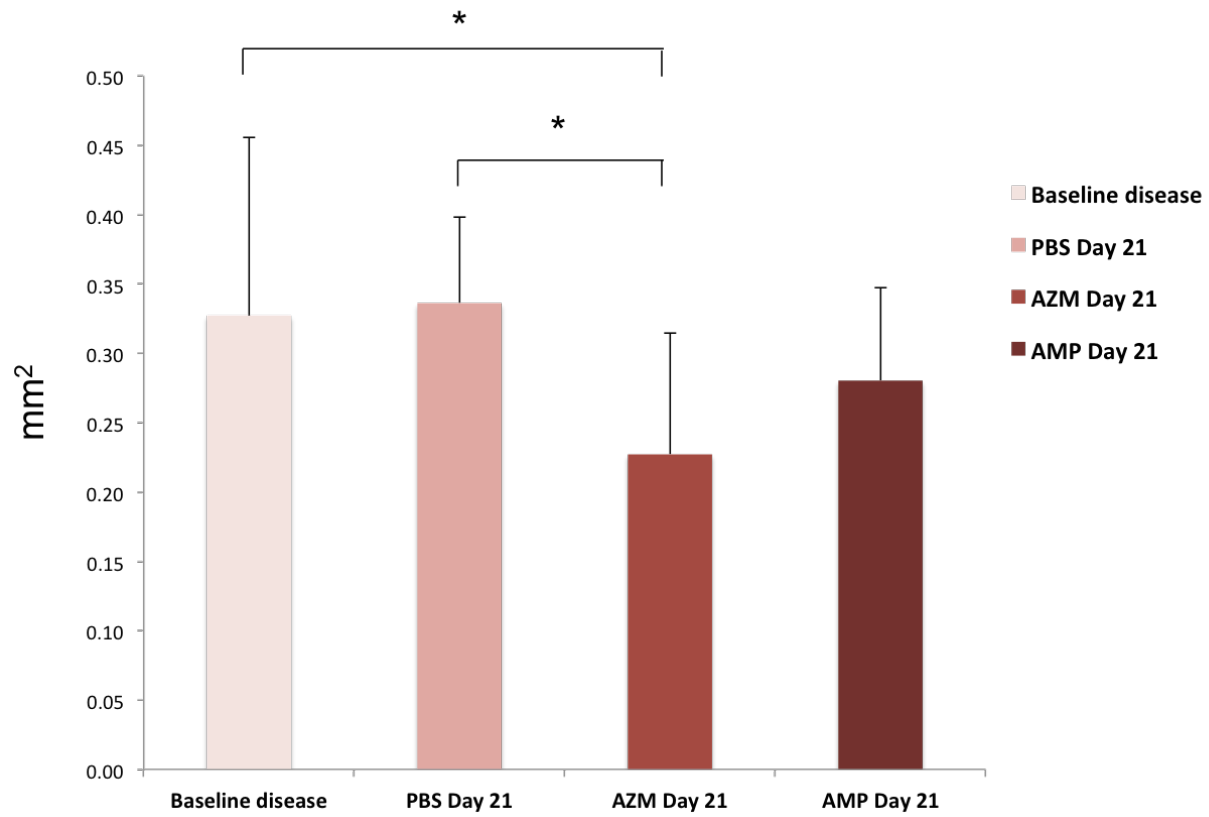


Figure 7: Extent of periapical lesion in mm². Azithromycin treated animals had significant decrease in lesion size. Vertical bar: SD, *: p<0.05.

In contrast to the results obtained with azithromycin, treatment with GdCl₃ and MCL failed to modulate the extent of periapical lesion size. As seen in (Fig. 8), no significant difference could be observed between GdCl₃ and PBS groups ($p>0.05$). Likewise, same findings were noticed in MCL and BL groups.

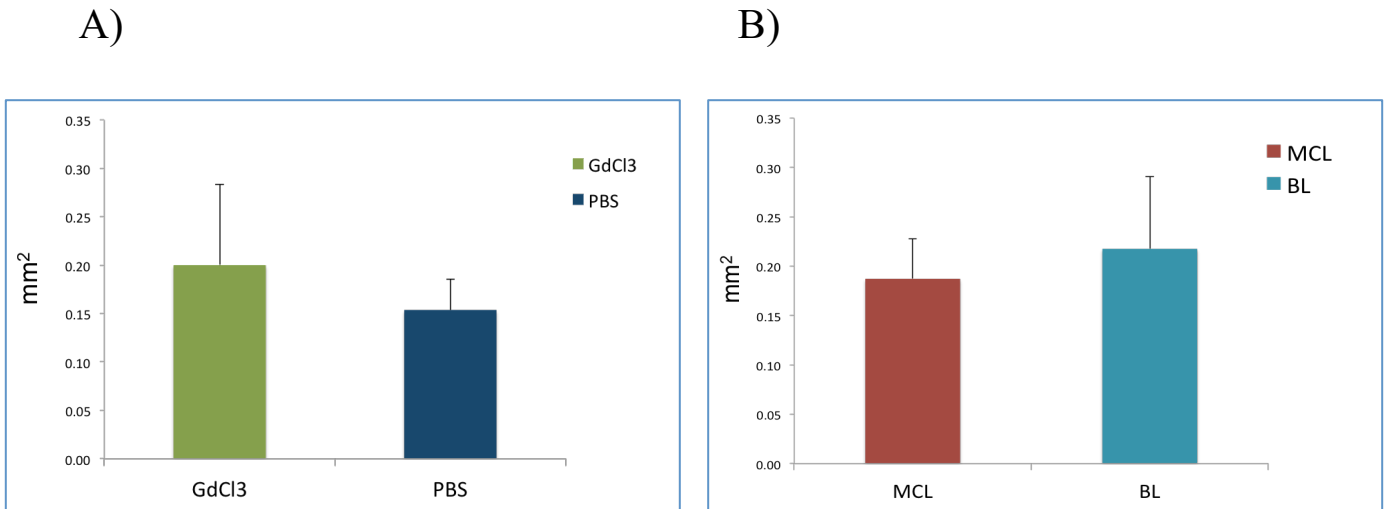


Figure 8: Quantification of bone loss in the periapical region (mm²).

A) Comparison between GdCl₃ and PBS groups. B) Extent of periapical lesion in MCL and BL groups.

We further pursue the investigation of potential mechanism of azithromycin-mediated down regulation of inflammation and attenuated wound healing of periapical lesions through histology, immunohistochemistry and gene expression analysis of the mice samples.

b) Histological Analysis

Periapical lesions are characterized by an infection-induced inflammation on the periradicular tissues. When the root canal system is exposed to bacteria and their by-products, a non-specific inflammatory response occurs leading to host immunological responses on the area (84-86). Initial inflammatory responses consist of infiltration of polymorphonuclear leukocytes (PMNs) and macrophages and later, T-cells and B-cells can be observed. While we observed the reduction of periapical lesion size on the uCT analysis, we sought to conduct histological and immunohistochemistry evaluation to determine the type of inflammatory infiltrating cells as well as the macrophage phenotype present in the periradicular tissues of day 10 (baseline disease) and day 21 (treatment endpoint) treated animals. Hemi-mandibles were processed for standard histology and stained with H&E. Samples were subjected to immunohistochemistry using the follow antibodies: 1) anti-mouse Mac2 antibody (total macrophage); 2) anti-mouse Ly6G antibody (neutrophil); 3) anti-mouse iNOS antibody (a marker of M1 macrophage); 4) anti-mouse Arg-1 antibody (a marker of M2 macrophage); 5) anti-mouse Osteocalcin (osteoblast); and 6) anti-mouse Cathepsin K (osteoclast).

At day 10, we could observe extensive periapical lesions with prominent infiltration of inflammatory cells in the lesion of all specimens (Fig. 9) using H&E

staining. A mix population of neutrophils, classically (M1) and alternatively (M2) activated macrophages was noted when immunohistochemistry was performed. At day 21, the same pattern of cell infiltration and localization was observed on the PBS (control) group with considerable amount of Ly6G+, Mac2+, iNOS+ and Arg-1+ cells overlapping (Fig.10). In contrast, both treatment groups, that are azithromycin and ampicillin, presented a decrease in neutrophils (Ly6G+) and pro-inflammatory (M1) macrophage (iNOS+) infiltration (Fig. 11, 12). Azithromycin treated group had a pronounced reduction in inflammatory cells and consequent decreased in periapical lesion size. Anti-inflammatory (M2) macrophages (Arg-1) were the predominant cell phenotype on the area. They were clearly separated from the other cell types and were located surrounding the margins of the lesion (Fig.11). Furthermore, osteocalcin + (osteoblast marker) cells were visualized lining the bone surface surrounding the periapical lesion in the azithromycin treated group, suggesting some bone regeneration (Fig. 13). Osteoblast could be visualized in certain ampicillin samples but were inconsistent compared to azithromycin group. No such cells were noted on the PBS (control), however, cathepsin K + (osteoclast marker) cells were present in PBS and ampicillin groups.

Cell enumeration analysis was not feasible due to cell clamping on the periapical area. Inflammatory cells presented as a mix population, especially on the control groups (day 10 and PBS), making it difficult to count and compare with azithromycin group.

The findings indicated that root canal infection is effective on the development of periapical lesions in mice at day 10. Additionally treatment with ampicillin and azithromycin are both effective on the reduction of periapical inflammation at day 21.

Even though ampicillin seems to reduce neutrophils and M1 macrophages infiltration surrounding the infected root, longer-term observation would be needed for the detection of bone regeneration. In contrast, animals treated with azithromycin demonstrated an enhanced periapical wound healing noticed by the recovered of bone on the area as well as the pattern and location of immune cells. These data suggest that azithromycin might be responsible for M2 polarization on the periapical lesion and helpful for accelerated wound healing.

Day 10: baseline disease

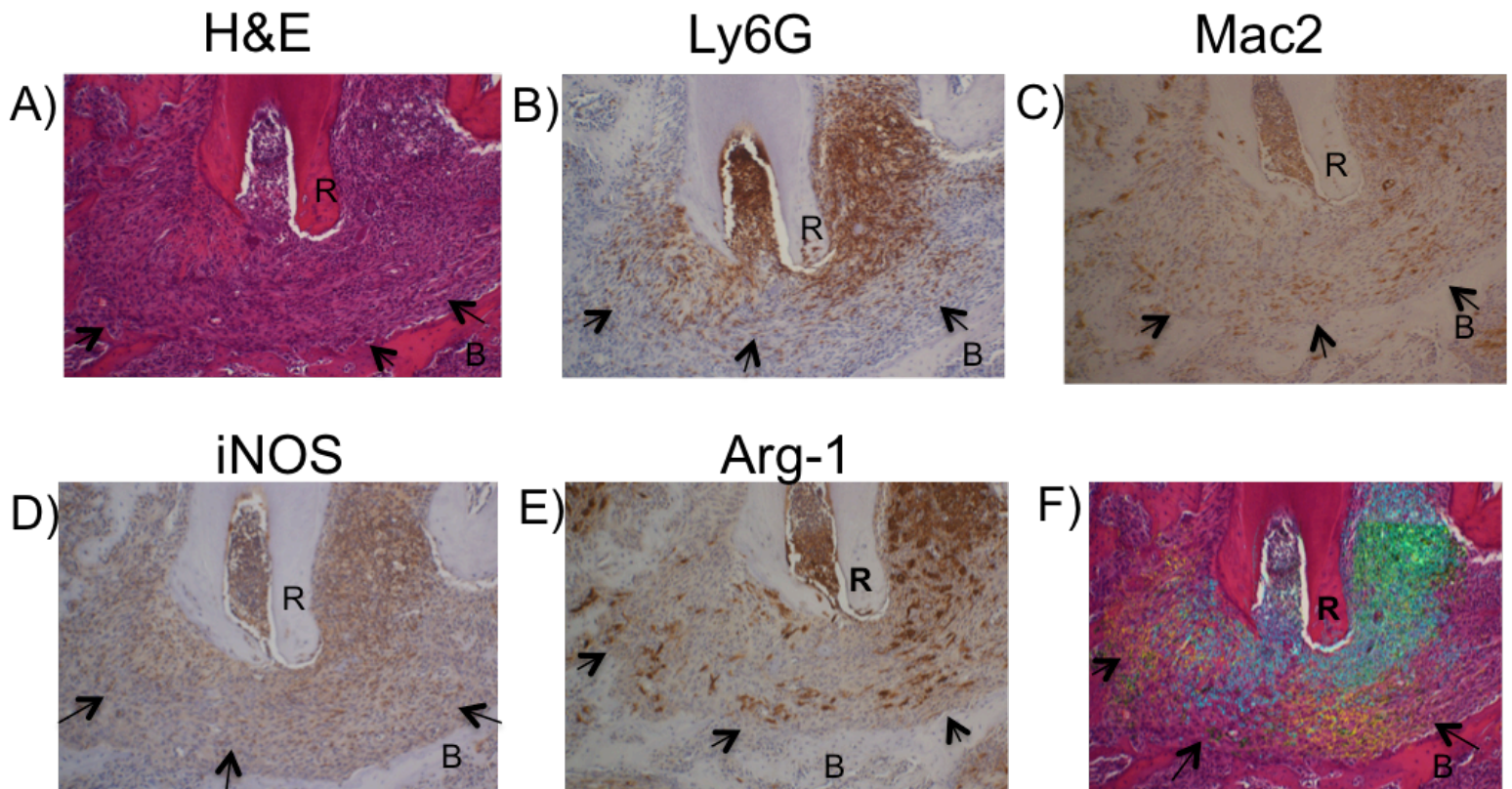


Figure 9: Representative images of histological sections of Day 10 (baseline disease) group: A) H&E, B) Ly6G (neutrophils), C) Mac2 (total macrophages), D) iNOS (M1) and E) Arginase 1 (M2) immunostaining. Neutrophils and M1 macrophages are clearly the predominant cells on these samples. F) Overlying of infiltrating cells; green= Arg-1+; yellow= iNOS+; blue= LY6G+. No specific location can be visualized. Cells are overlapping inside the lesion. R: root; B alveolar bone; arrows demarcate periapical lesion.

Day 21: PBS group

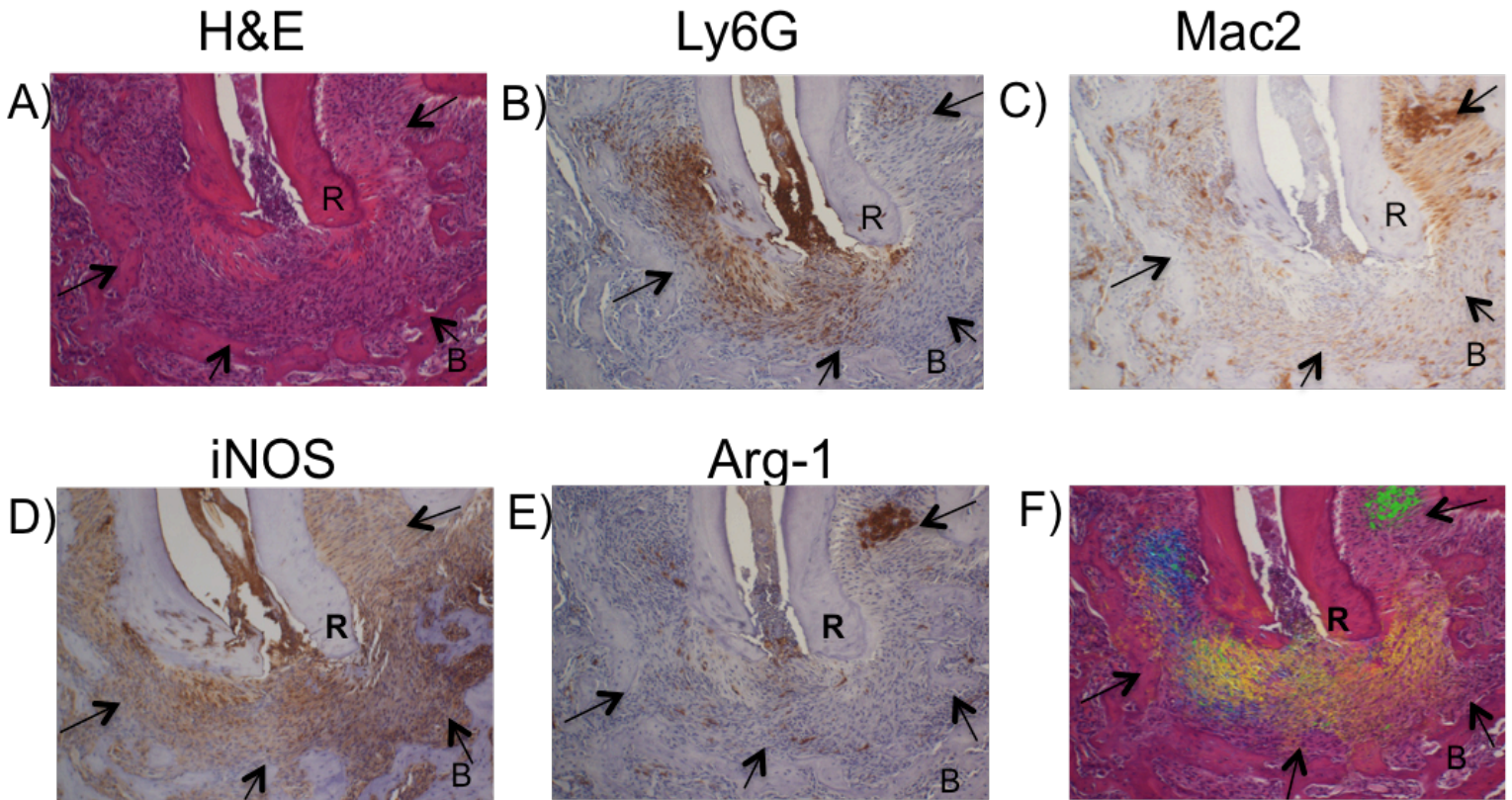


Figure 10: Representative images of histological sections of PBS group: A) H&E, B) Ly6G (neutrophils), C) Mac2 (total macrophages), D) iNOS (M1) and E) Arginase 1 (M2) immunostaining. Inflammatory cells are the most abundant. F) Overlying of infiltrating cells; green= Arg-1+; yellow= iNOS+; blue= LY6G+. Overlapping of neutrophils and pro-inflammatory macrophages is evident. R: root; B alveolar bone; arrows demarcate periapical lesion.

Day 21: Azithromycin Group

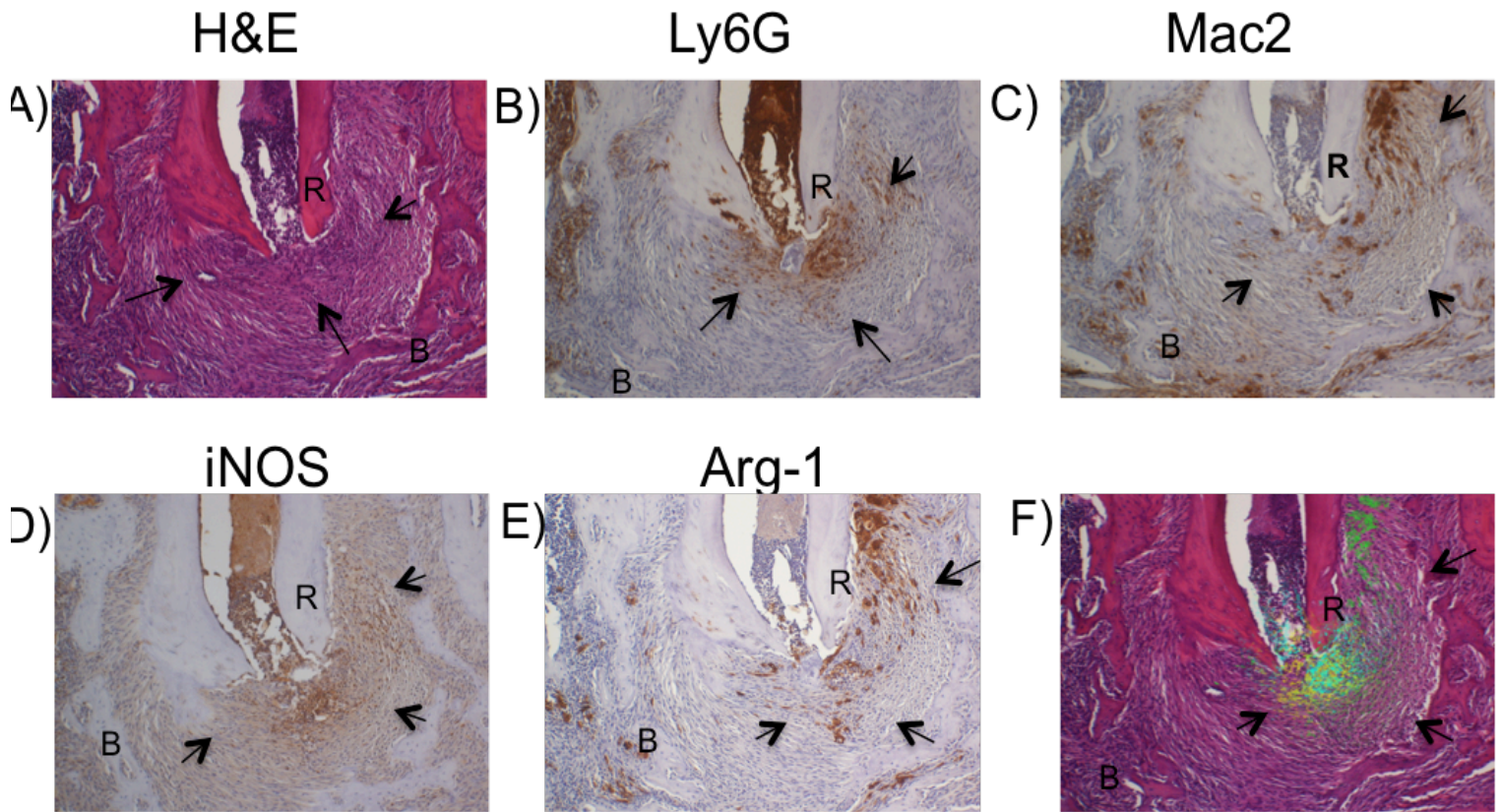


Figure 11: Representative images of histological sections of Azithromycin group:

A) H&E, B) Ly6G (neutrophils), C) Mac2 (total macrophages), D) iNOS (M1) and E) Arginase 1 (M2) immunostaining. Inflammatory cells are much less abundant than PBS group. M2 (Arg-1+) cells are the predominant cells surrounding the lesion. F) Overlaying of infiltrating cells; green= Arg-1+; yellow= iNOS+; blue= LY6G+. Distinct population of M2 macrophages can be observed. R: root; B alveolar bone; arrows demarcate periapical lesion.

Day 21: Ampicillin Group

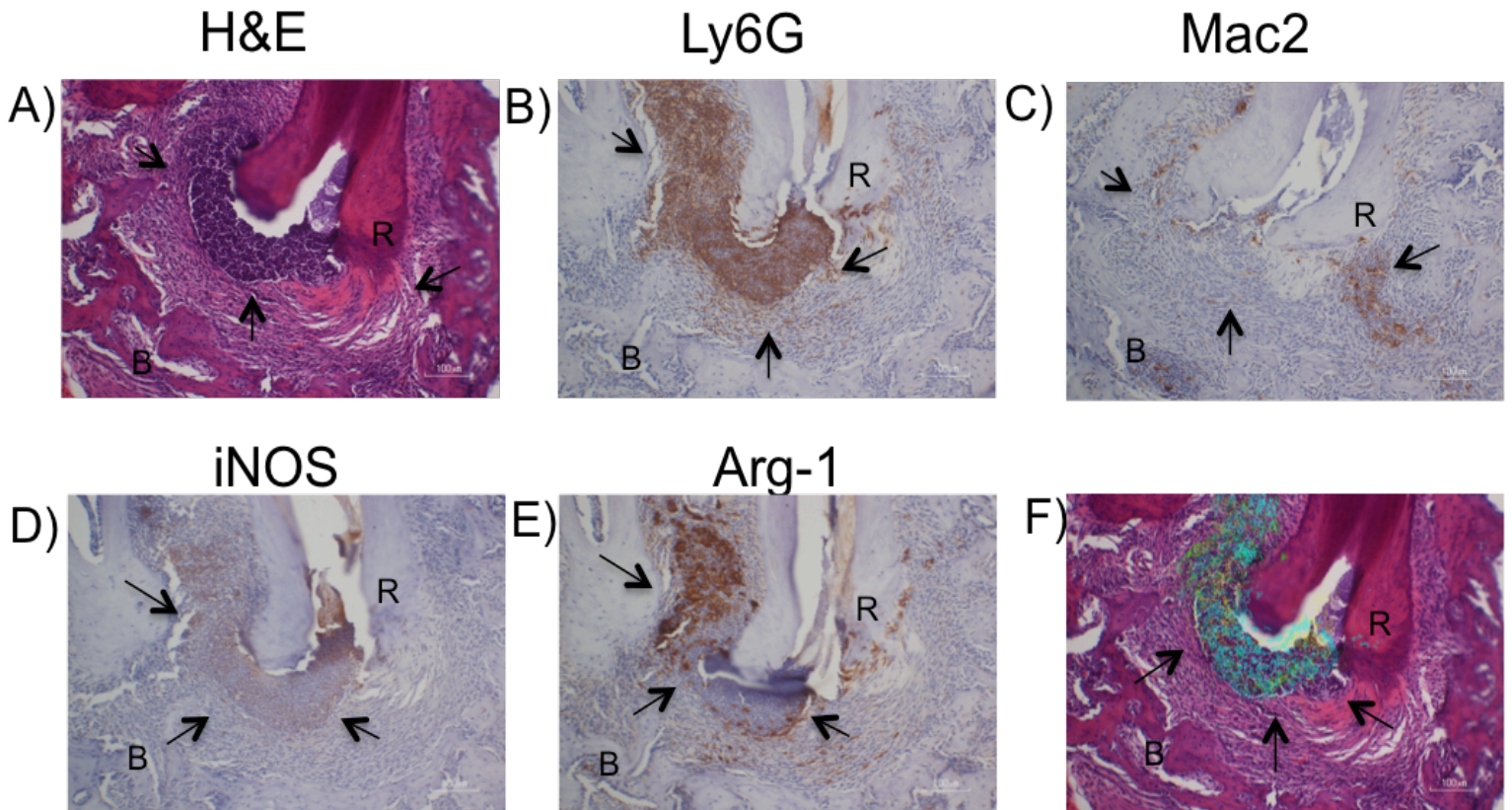


Figure 12: Representative images of histological sections of Ampicillin group:

A) H&E, B) Ly6G (neutrophils), C) Mac2 (total macrophages), D) iNOS (M1) and E) Arginase 1 (M2) immunostaining. Great amount of neutrophils as well as M1 and M2 macrophages. M2 (Arg-1+) cells surround the lesion. F) Overlaying of infiltrating cells; green= Arg-1+; yellow= iNOS+; blue= LY6G+. No distinct population can be observed as it was on AZM group. R: root; B alveolar bone; arrows demarcate periapical lesion.

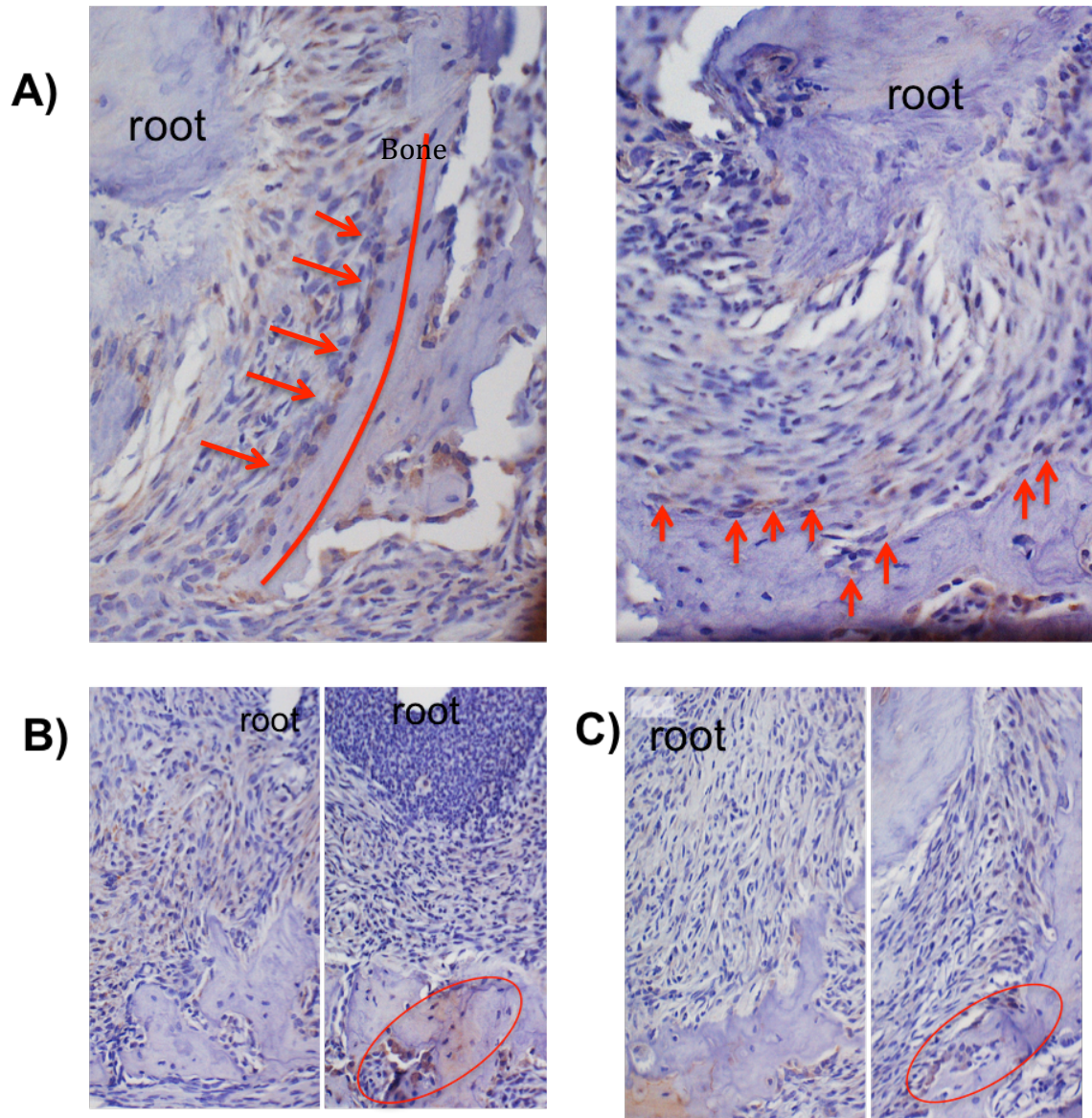


Figure 13: Representative immunohistochemistry of anti-mouse Osteocalcin in mice periradicular tissue: A) AZM group showing osteoblast cells lining the bone surrounding the periapical lesion. B) AMP group; C) PBS group. Both B and C lack osteocalcin+ cells. Some osteoblasts can be observed in the bone outside the periapical lesion.

c) Gene expression analysis:

In order to evaluate the expression level of several genes involved in the pathogenesis and wound healing of periapical lesions, we used the left hemi-mandibles of day 10 (baseline diseased), PBS, azithromycin and ampicillin groups. mRNA extraction was performed from the isolated bone block surrounding the root apices of mandibular first molar roots (more details are provided in the Material and Methods). Expression levels of genes involved in the inflammatory response, inflammasome, osteogenesis and wound healing as well as macrophage markers (refer to material and methods for full description of genes) were analyzed by Quantitative Real Time Polymerase Chain Reaction (RT-PCR) using GAPDH as internal control. The gene expression level of day 21 treatment groups were compared to the infected mice sacrificed at day 10= baseline disease control (Table 2).

mRNA ID	Well	Fold Up- or Down-Regulation			mRNA ID	Well	Fold Up- or Down-Regulation		
		PBS	AZM	AMP			PBS	AZM	AMP
GAPDH	A01	-1.00	-1.00	-1.00	Aim2	D01	-1.17	-1.08	1.24
Actb	A02	-1.45	1.28	-1.32	Casp1	D02	-1.42	-1.05	1.04
CXCI2	A03	-2.86	-2.28	-2.09	Nlrc4	D03	1.46	1.32	1.69
IL-10	A04	-2.24	-1.05	-1.54	Nlrp-1a	D04	-2.66	-1.30	-1.52
IL-17a	A05	-1.54	1.35	-1.16	Nlrp-3	D05	-1.65	1.31	-1.13
IL-1a	A06	-4.14	-1.89	-2.58	Myd88	D06	-1.27	-1.25	1.11
IL-1b	A07	-3.19	-1.73	-1.87	Ripk2	D07	-1.54	-1.16	-1.00
IFNg	A08	-1.14	-1.16	-1.04	Casp12	D08	-1.94	1.18	-1.07
CcL5	A09	-2.36	1.86	1.08	BMP2	E01	-1.18	-1.18	1.21
CCR1	A10	-1.15	-1.20	-1.03	BMP3	E02	-1.17	1.09	1.20
IL-1rn	A11	-2.36	-1.46	-1.91	Belap	E03	-7.63	-1.58	-2.42
IL-6	A12	-1.93	-1.84	-1.67	Col1a1	E04	-5.25	1.07	-1.72
PTGS2	B01	-1.25	-1.13	1.04	Spp1	E05	-3.62	1.30	-1.46
TNF	B02	-1.22	1.17	1.17	OPG	E06	1.01	-1.05	1.21
Ccl11	B03	-1.18	1.24	1.28	IL-4	F01	1.45	2.22	2.00
Lta(TNF-b)	B04	-1.02	-1.00	1.39	CSF-2	F02	1.78	-1.62	-1.25
NFKB-1	B05	-1.27	1.67	1.20	Fgf2	F03	1.27	-2.29	-1.51
Nos2	B06	-1.44	-1.06	1.16	CSF-1	F04	-1.28	-1.19	-1.00
CD86	C01	1.06	2.33	1.23	TGFb1	F05	-1.22	1.63	1.05
CD80	C02	1.77	1.65	4.96	Neg	F06	-1.36	-1.18	-1.22
CD163	C03	-1.11	-1.67	-2.24					
CD43	C04	1.23	-1.28	-1.15					
CCR2	C05	1.06	-1.57	1.05					
CX3CR1	C06	-1.09	-1.03	-1.33					
LY6C	C07	-1.85	1.46	1.04					

Table 2: Gene expression level of day 21 treatment groups. The gene expression levels were compared to day 10. Results are shown as fold up or down regulation comparing to baseline disease (day 10). Results in pink show fold change greater than 2. Results in blue demonstrate statistically significant fold change $p < 0.05$.

PBS (day 21 control group) presented a significant decreased ($p < 0.05$) in the expression of pro-inflammatory cytokines IL-1 β and IL-6 as well as CXCL2 chemokine and osteocalcin (Bglap) protein. Likewise, mRNA expression of IL-1 β , IL-1rn, CCL5, IL-10 NLRP-1a, COL1a1 and SPP1 (osteopontin) were also down regulated ($p > 0.05$) in a meaningful way when compared to baseline diseased mice (Table 3). IL-1 β and IL-6 have been implicated in bone resorption in the periapical lesion (87, 88) and the down regulation of those genes and the genes related to the inflammasome suggest that the periapical lesion at day 21 is no longer on the acute phase of inflammation.




PBS Group	Gene	Regulation	Fold Change
Inflammatory response	IL-1 β		-4.14 *
	IL-1 β		-3.19
	CXCL2		-2.86 *
	CCL5		-2.36
	IL-1rn		-2.36
	IL-6		-1.93 *
	IL-10		-2.24
Inflammasome	NLRP-1a		-2.66
Osteogenesis	Bglap		-7.63 *
	Col1a1		-5.25
	Spp1		-3.62

Table 3: List of genes on PBS group with fold change > 2 compared to baseline disease. Arrows mean down regulation. * Indicates statistical significant difference ($p < 0.05$).

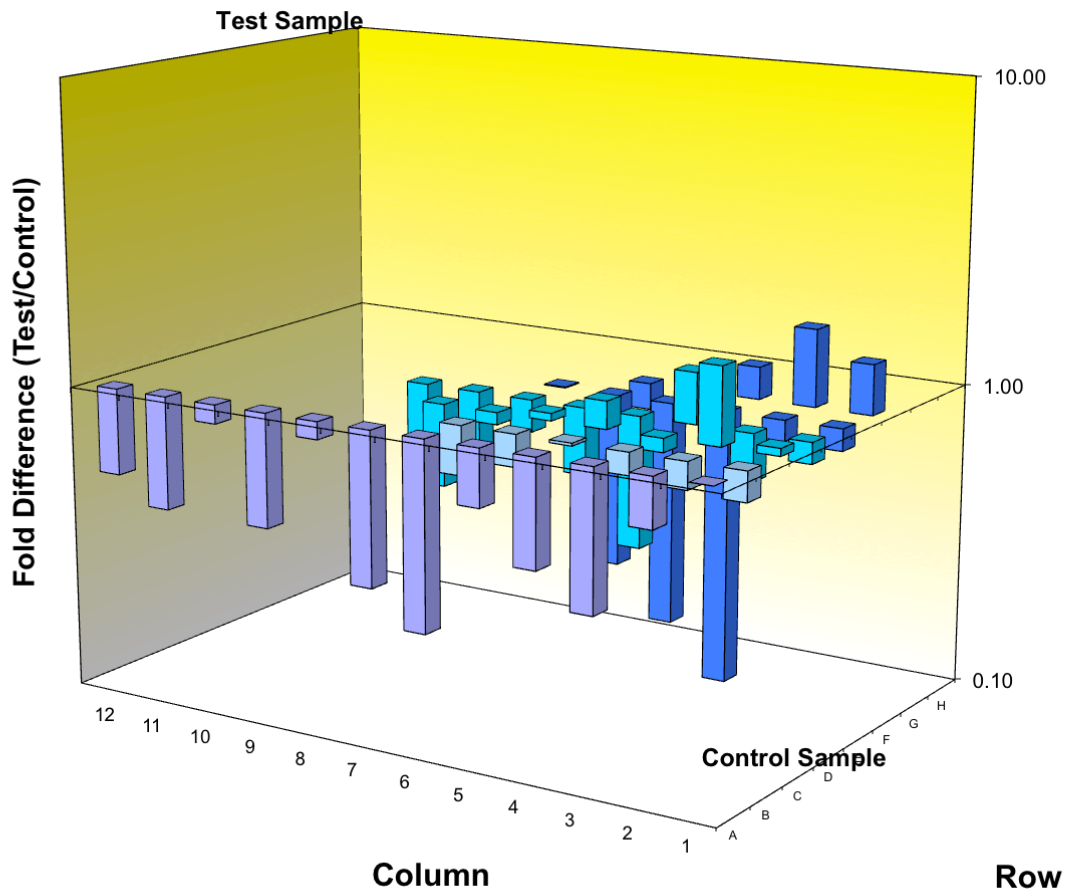


Figure 14: PBS gene expression data arranged in a 3D profile. Rows A and B: inflammatory response; C: macrophage markers; D: inflammasome; E: osteogenesis; F: wound healing.

Azithromycin group showed a decrease in expression of pro-inflammatory cytokine IL-6 and chemokine CXCL2. Colony stimulating factor 2 (CSF2), together with the mentioned genes, had a significant down regulation in expression when compared to baseline disease ($p < 0.05$). Fibroblast growth factor 2 (FGF2) was also down regulated ($p > 0.05$). An interesting finding was the up regulation of the surface marker CD86 and the cytokine IL-4 (Table 4). CD86 is a co-stimulatory molecule that serves as ligand for activation of T-lymphocytes (89). IL-4 has been reported to down regulate the expression of IL-1 β (90) and most importantly to our study, to activate the macrophage polarization to an M2 phenotype (91).

AZM Group	Gene	Regulation	Fold Change
Inflammatory response	CXCL2	↓	-2.28 *
	IL-6		-1.84 *
Macrophage marker	CD86	↑	2.33
Wound Healing	CSF2	↓	-1.62 *
	FGF2		-2.29
	IL-4	↑	2.22

Table 4. List of gene expression showing relevant fold change. CD86 and IL-4 were up regulated and FGF2 was down regulated ($p > 0.05$). Statistical significant difference (*) could be observed on the down regulation of CXCL2, IL-6 and CSF2 ($p < 0.05$).

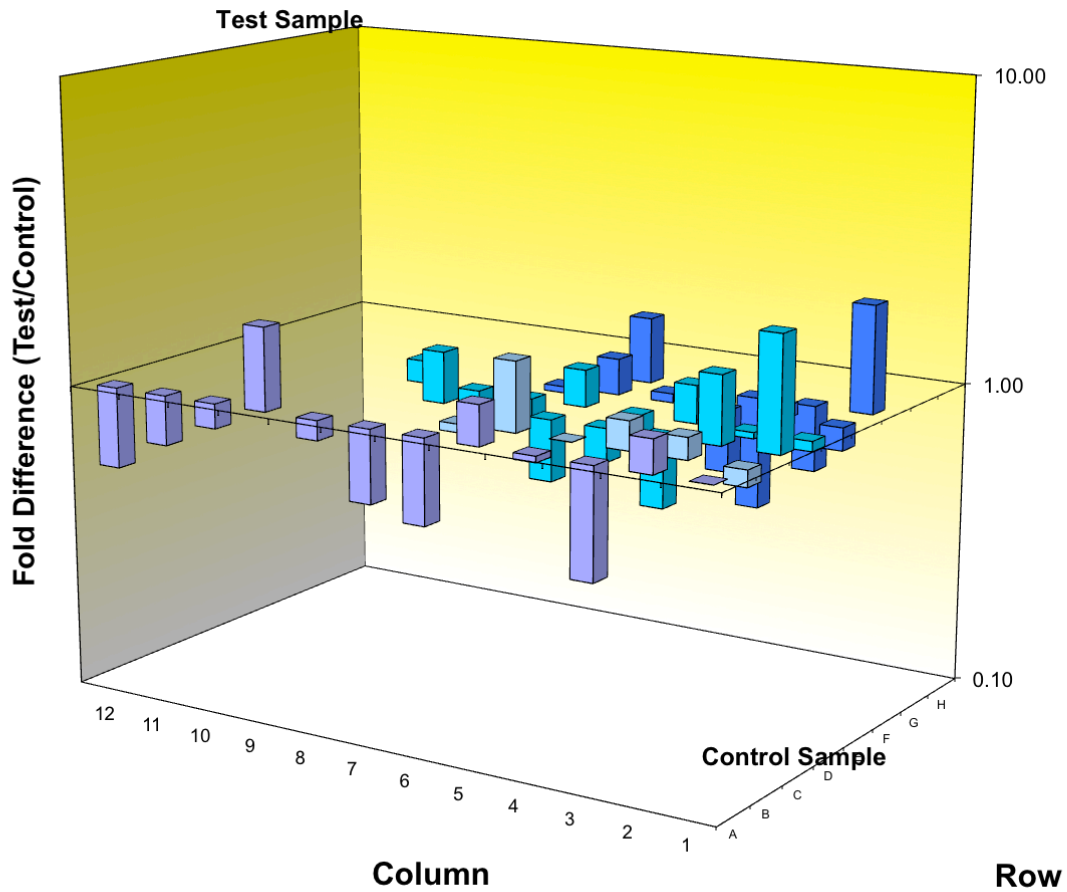


Figure 15: AZM gene expression data arranged in a 3D profile. Rows A and B: inflammatory response; C: macrophage markers; D: inflammasome; E: osteogenesis; F: wound healing. Up regulation of CD86 and IL-4 is clearly noted.

When examining the gene profile of ampicillin group, the genes that were down regulated with significance were similar to the PBS group, that is CXCL2, IL-6, CX3CR1 ($p < 0.05$), IL-1 β and Bglap ($p > 0.05$). A substantial fold increase was observed for the M1 macrophage marker CD80 when compared to baseline disease (table 5).



AMP Group	Gene	Regulation	Fold Change
Inflammatory response	IL-1 β		-2.58
	CXCL2		-2.09 *
	IL-6		-1.67 *
	CX3CR1		-1.33 *
Osteogenesis	Bglap		-2.42
Macrophage marker	CD80		4.96

Table 5. List of gene expression showing relevant fold change in AMP group. Down regulation of CXCL2, IL-6, CX3CR1 ($p > 0.05$) IL-1 β and Bglap ; and up regulation of CD80 ($p > 0.05$) are shown. (*) Indicates statistical significant difference.

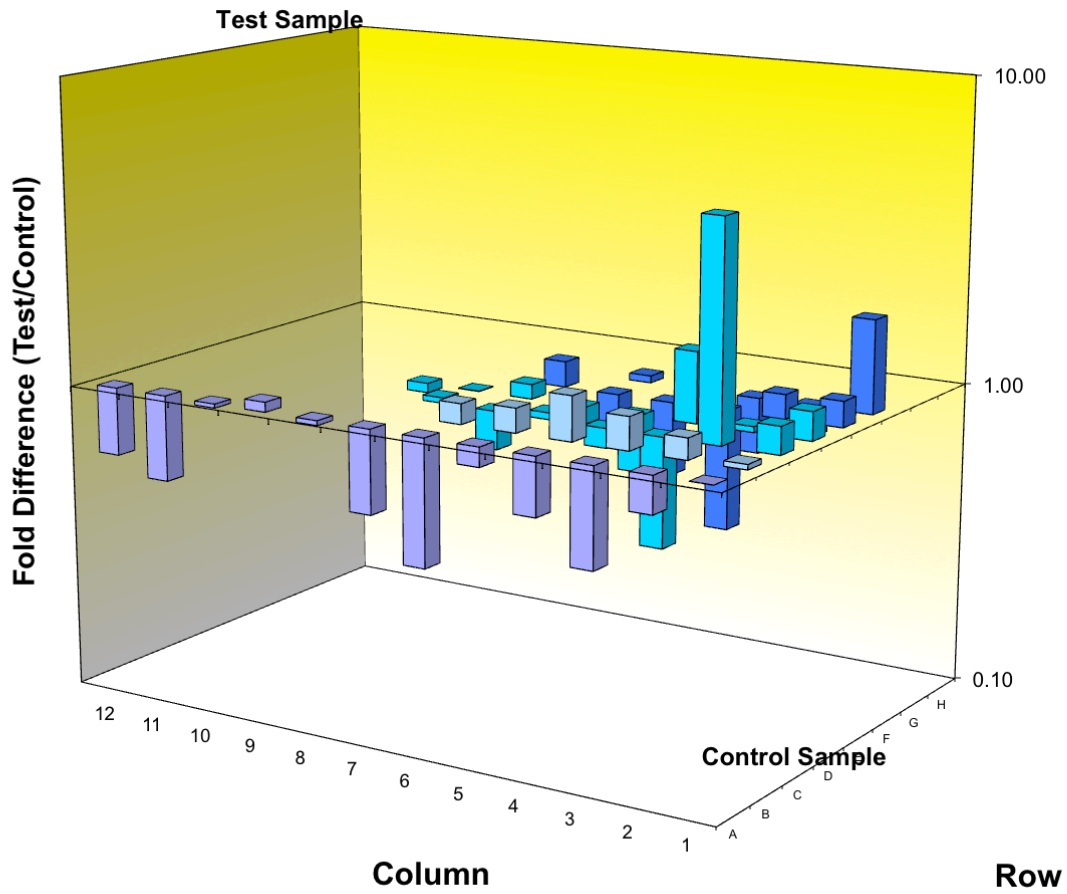


Figure 16: AMP gene expression data arranged in a 3D profile. Rows A and B: inflammatory response; C: macrophage markers; D: inflammasome; E: osteogenesis; F: wound healing. Up regulation of CD80 is visibly noticeable.

In order to evaluate whether the gene expression of the azithromycin treatment was corroborating to our immunohistochemistry findings on the wound healing and bone regeneration of the periapical lesions, we compared the data set of AZM and AMP groups to PBS group (day 21) (Table 6).

mRNA ID	Well	Fold Up- or Down-Regulation		mRNA ID	Well	Fold Up- or Down-Regulation	
		AZM	AMP			AZM	AMP
GAPDH	A01	-1.00	-1.00	Aim2	D01	1.09	1.45
<u>Actb</u>	A02	1.86	1.10	Casp1	D02	1.36	1.48
CXCL2	A03	1.25	1.37	Nlrc4	D03	-1.11	1.15
IL-10	A04	2.14	1.45	Nlrp-1a	D04	2.05	1.75
IL-17a	A05	2.08	1.33	Nlrp-3	D05	2.17	1.45
IL-1a	A06	2.18	1.61	Myd88	D06	1.02	1.42
IL-1b	A07	1.84	1.71	Ripk2	D07	1.33	1.53
<u>IFNg</u>	A08	-1.02	1.10	Casp12	D08	2.29	1.81
Ccl5	A09	4.40	2.54	BMP2	E01	-1.00	1.43
CCR1	A10	-1.04	1.12	BMP3	E02	1.28	1.40
IL-1rn	A11	1.62	1.24	<u>Bglap</u>	E03	4.84	3.15
IL-6	A12	1.05	1.15	Col1a1	E04	5.60	3.06
PTGS2	B01	1.10	1.30	Spp1	E05	4.72	2.48
TNF	B02	1.44	1.43	OPG	E06	-1.05	1.20
Ccl11	B03	1.46	1.51	IL-4	F01	1.53	1.38
<u>Lta(TNF-b)</u>	B04	1.02	1.42	CSF-2	F02	-2.89	-2.22
NFKB-1	B05	2.13	1.52	Fgf2	F03	-2.91	-1.92
Nos2	B06	1.36	1.68	CSF-1	F04	1.08	1.28
CD86	C01	2.20	1.16	TGFb1	F05	1.98	1.28
CD80	C02	-1.07	2.80	<u>Neg</u>	F06	1.15	1.11
CD163	C03	-1.51	-2.02				
CD43	C04	-1.57	-1.42				
CCR2	C05	-1.66	-1.01				
CX3CR1	C06	1.06	-1.21				
LY6C	C07	2.70	1.92				

Table 6: Gene expression level of AZM and AMP. The gene expression levels were compared to PBS group. Results are shown as fold up or down regulation. Results in pink show fold change greater than 2. Results in blue demonstrate statistically significant fold change $p < 0.05$.

Azithromycin group had an exponentially increase in the gene expression of the osteogenic genes Bglap, Coll1a1 and Spp1. Expression of TGFβ mRNA showed a significant increase ($p < 0.05$) when compared to PBS control. The gene expression of anti-inflammatory molecules IL-10 and IL-1Ra were up regulated, substantiating the hypothesis of M2 macrophage polarization by azithromycin. The gene expression of the ampicillin treated animals had similar up regulation of Bglap, Coll1a1 and Spp1 however, in far less extent than AZM group (Fig. 17).

A) AZM gene profile

B) AMP gene profile

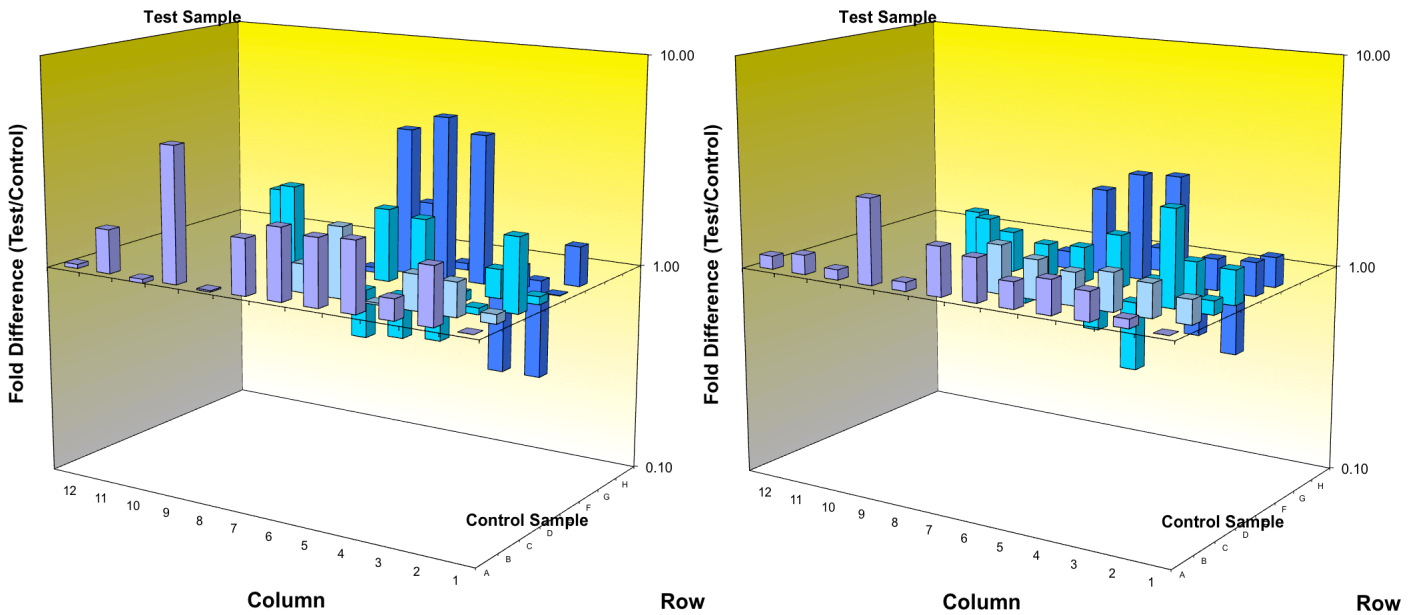


Figure 17: 3D profile of gene expression of AZM and AMP treated mice compared to day 21 PBS control. Expression of osteogenic genes noted in dark blue on the E row. Fold difference of gene expression is noticeably up regulated in the AZM group.

Expression patterns of RANKL mRNA (Fig.18) showed no difference amongst the groups.

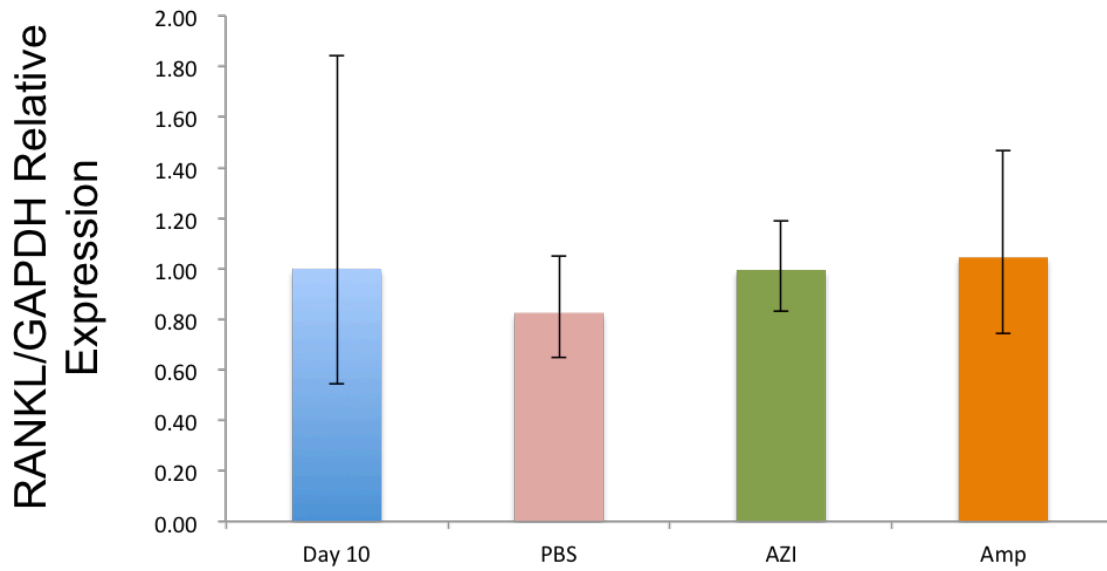


Figure 18: RANKL expression in periapical lesions. RT-PCR results showing the change in relative gene expression of RANKL mRNA to GAPDH (internal control) in all treatment groups. No significant difference was noted between the groups.

Additionally, we have examined whether azithromycin modulate NF- κ B activation and pro-inflammatory cytokine expression and nitric oxide production *in vitro*. The data obtained from the effect of AZM on the expression of pro-inflammatory cytokines IL-1 α and IL-1 β , as well as nitric oxide production were compared to AMP.

3. NF- κ B reporter assay

The luciferase reporter assay is broadly used as a tool to study gene expression at the transcriptional level. NF- κ B (nuclear factor kappa B) is the key transcription factor for macrophage inflammatory responses (92). To evaluate the effect of azithromycin in the level of NF- κ B gene expression NF- κ B Luciferase Stable RAW 264.7 cells were used. The cells were pre-incubated with azithromycin for 1 hour, stimulated with LPS for 12 hours. Then the cells were lysed and the relative luciferase activity was measured. The luciferase activity was decreased when cells were stimulated with AZM 50uM and AZM 25uM while 12.5uM AZM failed down regulation of NF- κ B (Fig. 19). This data suggests that azithromycin is capable of modulate NF- κ B activation.

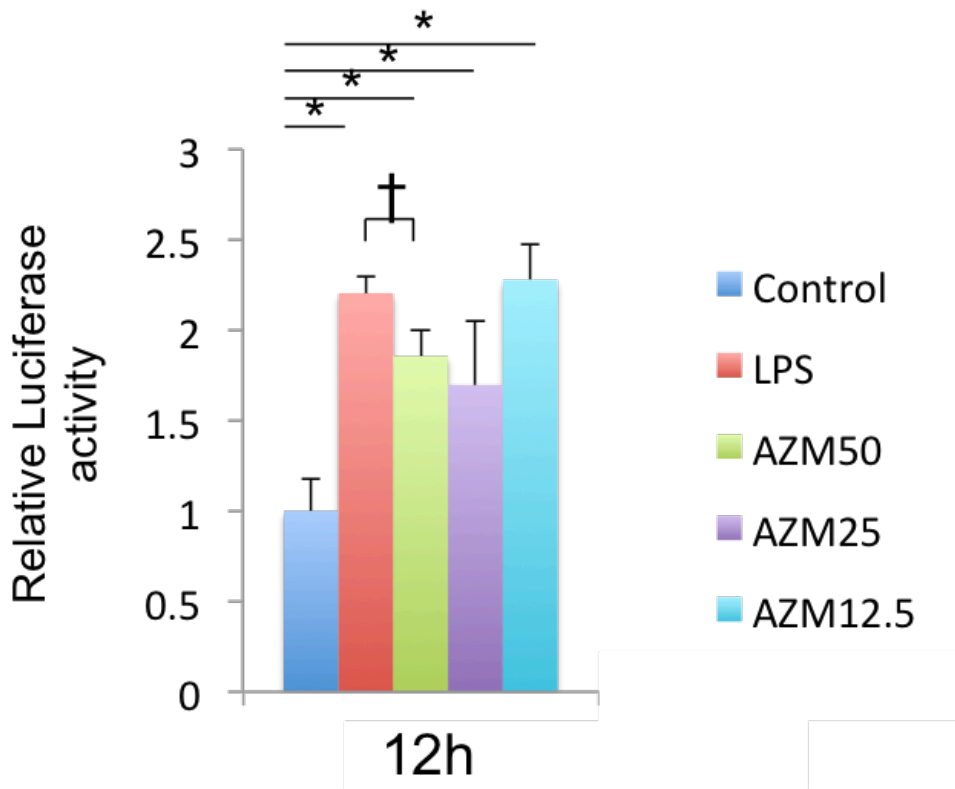


Figure 19: Luciferase activity upon stimulation with 3 different concentrations

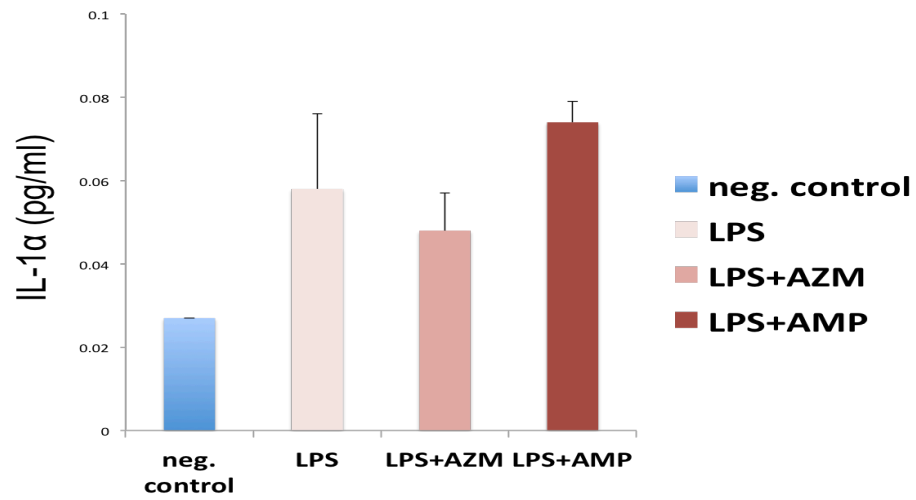
(12.5uM; 25uM and 50uM) of AZM * Indicates significant statistical difference

p< 0.05 (vs control), †: p<0.05 (vs LPS).

4. Cytokine expression of stimulated peritoneal macrophages

In order to assess the effect of the antibiotics on the production of pro-inflammatory cytokines IL-1 α and IL-1 β , peritoneal macrophages were stimulated with LPS in the presence/absence of azithromycin and ampicillin. Culture supernatants were measured by ELISA (pg cytokine/ml of culture supernatant). As shown in Fig. 20 ampicillin showed a consistent up-regulation on the levels of IL-1 α and IL-1 β . The up-regulation of pro-inflammatory cytokines has been reported by Karlstrom *et al* (93) corroborating our findings. Azithromycin stimulated cells had a slight decrease in the production level of IL-1 α while IL-1 β expression but did not differ from the cells stimulated with LPS alone.

A)



B)

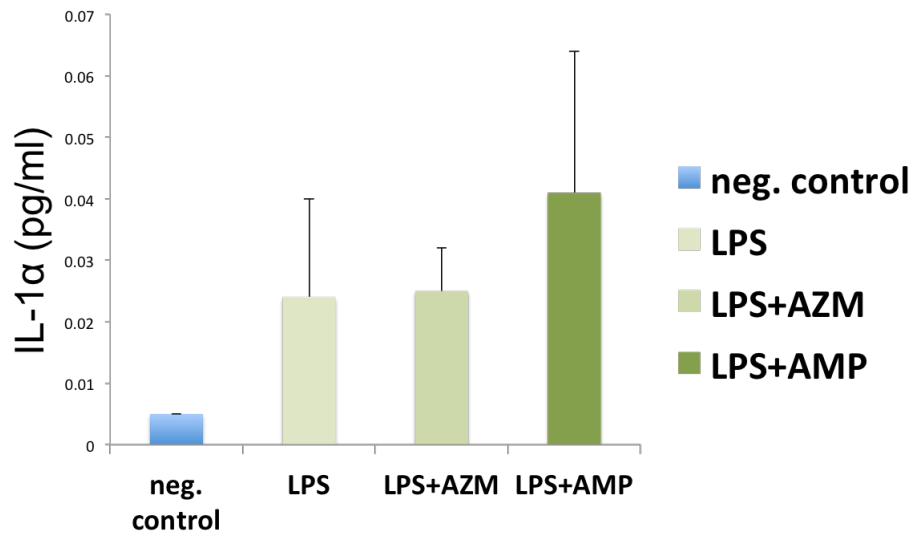


Figure 20: A) IL-1 α and B) IL-1 β expression in response to antibiotics stimulants *in vitro* by peritoneal macrophages. Results are expressed as picograms of cytokine/milligram of supernatant. No statistical differences were observed.

5. Nitric Oxide production by stimulated peritoneal macrophages

iNOS, has been advocated as an important biomarker of inflammation, as its over-expression leads to extreme production of nitric oxide, a free radical that plays an important role on the immune system (94). M1 but not M2 polarized macrophages exhibit up-regulation of iNOS (70). Azithromycin is known to shift the polarization to an alternatively activated (M2) phenotype and to test that veracity we stimulated pre-treated (azithromycin and ampicillin) peritoneal macrophages with LPS. The production of nitric oxide (NO) by activated macrophages was measured after 12 hours. Down-regulation of iNOS expression (\square 76%) was clearly noticed in the azithromycin treated macrophages ($p < 0.05$). Treatment with ampicillin decreased iNOS production but it was not statistical significant as presented in Fig.21.

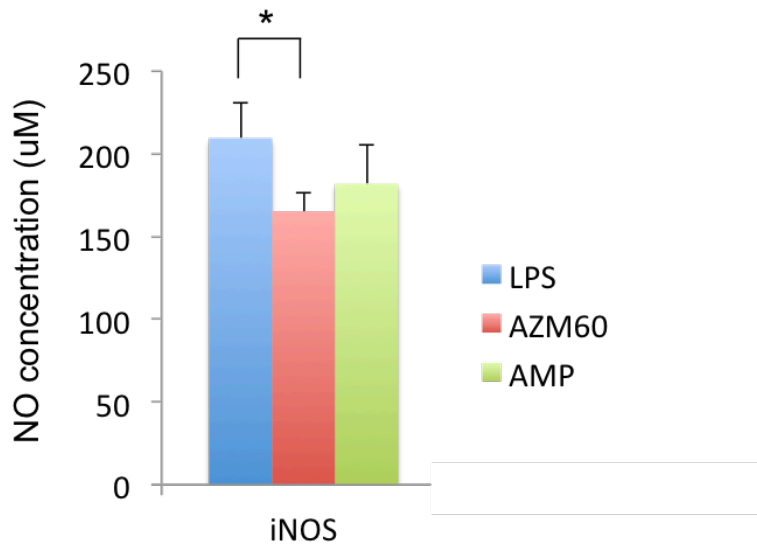


Figure 21: iNOS expression when stimulated macrophages are exposed to AZM 60uM and AMP 100ug/ml. AZM down -regulated expression of iNOS. * Indicates significant statistical difference ($p < 0.05$).

Discussion

The pathophysiology of the pulp and periradicular tissues has been well studied and documented over the years. The pulp tissue is encased in a hard matter with almost no collateral circulation making it difficult to regenerate after injury. Injuries to the pulp can be caused by dental procedures like crown preparation, orthodontic treatment and bleaching. However the most damage is caused by caries that left untreated can lead to rapid pulp inflammation, degeneration and necrosis. Infection of the root canal will cause an immunoinflammatory reaction on the periapex and need for root canal treatment.

A periapical lesion is an infection-induced inflammation that surrounds the tooth root resulting in the formation of granulomatous tissue and the destruction of bone in the area. The disease initiates with bacterial infection into the root canal system and its progression is also affected by host factors.

Despite all the new technology and emerging endodontic armamentarium, the success rate of root canal treatment remains unchanged (14, 15). The presence of pre-operative lesion and/or host immunosuppression decreases the prognosis even further. For example, diabetic patients have lower success rates after endodontic treatment, suggesting the importance of host factors on this disease (16, 95). However, periradicular wound healing is not completely understood thus a detailed investigation of the regulating molecular mechanisms is essential in order to develop rational therapeutic approaches that improve the healing of periapical lesions.

This study was based on the hypothesis that induction of M2 macrophage polarization will promote wound healing and induction of bone formation in mouse periapical lesions. Our primary focus was to determine the best method to induce that

polarization. We found that azithromycin is a practical choice to shift the macrophage polarization from a pro-inflammatory M1 to an anti-inflammatory M2 phenotype *in vitro*. Our *in vivo* studies showed that systemic treatment with azithromycin after pulp infection reduces the size of periapical lesion. This report is the first finding on pro-resolving M2 macrophage polarization during periapical wound healing.

The effect of proposed treatments on M1 and M2 macrophages

Since alternatively activated (M2) macrophages have been characterized more than two decades ago (96), they have been shown to play crucial role in the resolution of the inflammatory responses and tissue remodeling in areas of injury. According to Sterns *et al* macrophages constitute the majority of the cells in periapical granulomas (28) and a shift of their polarization towards the anti-inflammatory (M2) phenotype could assist the wound healing in the periapical lesions. Therefore, we began by investigating the optimal treatment for macrophage polarization. We based our animal preliminary study in the findings that gadolinium chloride (GdCl₃) and mannosylated clodronate liposome (MCL) selectively deplete M1 and M2 macrophage population respectively (56). C57BL/6J mice were injected with either GdCl₃/PBS control or MCL/BL control and, at the end of the treatment schedule blood samples were subjected to flow cytometry (FACs) analysis to confirm macrophage polarization. This methodology was chosen because flow cytometry can rapidly analyze several characteristics of cells and give us qualitative and quantitative information (97). GdCl₃ was capable of depletion of M1 macrophages, however no difference could be observed in its control group (PBS) (Fig.1). We believe that incomplete depletion could be attributed to the route of administration of the solution. M1

depletion in rats using intravenous injections in the tail vein reported a repopulation of M1 macrophages as early as 3 days (98). The intra-peritoneal injection of GdCl₃ might not have been effective enough to keep the M1 depletion in the same schedule as suggested by other studies (56, 98). Mannosylated clodronate liposome successfully depleted M2 macrophages as reported by Miron *et al.* However blank liposome (BL) was unpredictably more efficient on reducing both M1 and M2 macrophages (Fig. 1). This can be explained by the study from Rooijen *et al* that suggested that PBS or saline liposomes are not the correct control for liposome experiments. Healthy animals should be used as controls (99) once blank liposomes can block phagocytosis for a period of time (100). Since this point has not been concluded yet we decided to exclude this approach from our study.

On the other hand, azithromycin consistently shift the macrophage polarization to M2 phenotype *in vitro* as shown on Fig. 2 and Fig.3. These data coincide with a study by Murphy *et al*, in which they reported increased quantities of cells exhibiting M2 markers when a macrophage cell line was treated with azithromycin (70). Our data shows that primary peritoneal macrophages stimulated with azithromycin had an increase in CD206 expression, a surface marker indicative of anti-inflammatory phenotype; and decreased in CD68, a surface marker for pro-inflammatory M1 macrophages. Zhang *et al* showed same results *in vivo* (101). Treatment with ampicillin had no effect on M2 polarization under LPS stimulation.

The Effect of Azithromycin on the Extent of mouse periapical lesions

We investigated the effect of azithromycin treatment on the extent of periapical lesions in mice. Pulp exposure and infection were performed in young adult mice (6 weeks of age) and well-developed periapical lesions could be observed after 10 days (control group). Mice were then treated with azithromycin and ampicillin having PBS as control. Our results from uCT analysis showed that animals treated with azithromycin presented a decrease in size of periapical lesions exhibiting statistically significant difference when compared to PBS group ($p < 0.05$) (Fig. 5, 6, 7). In addition, the lesions were reduced when compared to day 10 ($p < 0.05$). As the lesion reached its peak at day 14 according to Kawashima and Stashenko (101) and remain stable between days 15 and 30 (26), we estimated that azithromycin stimulated bone recovery in the area at day 21. The decreased in inflammatory infiltrate in azithromycin group when analyzed by histology and immunohistochemistry might represent resolution of the inflammation and wound healing in the area. In similar way, Piancentini *et al* found reduction of airway neutrophil infiltration in asthmatic children after treatment with azithromycin (102). The anti-inflammatory effect of AZM and macrolides in general seems to be associated with decrease of pro-inflammatory cytokines causing the inhibition of neutrophil chemotaxis (103, 104). The greater amount of Arginase 1 + cells found surrounding the periapical lesions and lower quantity of iNOS+ in the AZM group are consistent with M2 macrophages polarization (105, 106). On the other hand, generation of nitric oxide (NO) is a characteristic of pro-inflammatory immune cells such as neutrophils and M1 macrophages (107). Even though nitric oxide production is necessary for bacteria killing, it triggers tissue destruction at the site of inflammation (108). Lin *et al* correlated NO to

osteoblast apoptosis in periapical lesion (109), while Gyurko *et al* demonstrated decreased amount of osteoclasts in the femur of iNOS KO compared to WT mice. The authors suggested that iNOS is an important signal for osteoclast differentiation (110). In our study we found osteoblast cells lining the bone surface surrounding the periapical lesion in the azithromycin treated group. In contrast, osteoclast cells were lining the bone surface in the baseline disease and PBS groups. Our findings can be validated by the studies mentioned above as the iNOS + cells can be visualized in greater amount on the latter groups. The presence of considerable iNOS+ cells overlapping Ly6G+ and Arg-1+ and Mac2+ cells on the periradicular tissues of baseline disease group as well as on PBS and ampicillin groups suggest the development of a chronic inflammation on the periapex, known as periapical granuloma (26, 27). It is well reviewed in the literature that chronic periapical lesion contains a dense accumulation of polymorphonuclear (PMN) leukocytes, lined by granulomatous tissue containing lymphocytes, macrophages and plasma cells (8, 22, 86). It is important to remember that cells composing the chronic periapical granuloma (asymptomatic apical periodontitis; AAE terminology) are not static and can change their profile at any point causing a reorganization process.

The down regulation of pro-inflammatory genes IL-6, CXCL2 and colony stimulating factor 2 (CSF2) and increased expression of IL-4 in the azithromycin treated group when compared to baseline disease group reiterates our hypothesis that M2 polarization can promote wound healing. Several authors have demonstrated production of IL-6 by the periradicular tissues (111, 112). IL-6 mediates the acute phase of inflammation and induces bone resorption by recruiting osteoclasts to the site of inflammation (113, 114). Huang *et al* and Balto *et al* demonstrated controversial findings

where they found IL-6 to be protective against bone resorption in the periapical lesion of IL-6^{-/-} mice (115, 116). CSF2 also known as granulocyte-macrophage colony-stimulating factor (GM-CSF) attracts pro-inflammatory macrophages to the site of inflammation, also confirmed in periapical lesion (113). Khan *et al* described a decrease in GM-CSF in LPS-stimulated human macrophages treated with azithromycin (69). It has been reported that IL-4 reduces the levels of TNF- α , IL-1 β and prostaglandin E2 (117), however Sasaki *et al* demonstrated that IL-4 did not suppress infection-stimulated bone resorption in mouse periapical lesion (31). PBS group showed a decrease in expression of pro-inflammatory genes suggesting a chronic and not acute phase of the inflammatory process in the area. Likewise, down regulation of pro-inflammatory genes were observed in ampicillin group, however the up regulation of CD80, a M1 macrophage marker suggests that wound healing is much slower than detected in azithromycin group.

A parallel comparison of gene expression was performed using the PBS group as control. Both AZM and AMP groups expressed up regulation of the osteogenic genes Bglap (osteocalcin), Col1a1 and Spp1 (osteopontin) with AZM group showing the greatest increase. Maeda *et al* found osteogenic markers, like osteocalcin and osteopontin, in human chronic apical lesions suggesting the potential contribution to osseous healing after root canal treatment (118). In our study, the osteogenic markers were increased without endodontic treatment proposing the role of azithromycin in the wound healing. Additionally, OPN-deficient mice had significantly increased in bone loss after pulp exposure and infection (119). The up-regulation of IL-10 expression reiterates the findings by Sasaki *et al* that demonstrated the role of IL-10 in infection-stimulated inflammatory responses suppression, including bone resorption (31). RANKL has been

recognized to have an critical role in osteoclastogenesis and it was showed to decrease after day 14 of pulp exposure in rats (120). Our results did not show this decrease. Day 21 groups had about the same level of RANKL mRNA gene expression when compared to day 10 (baseline disease).

NF- κ B reporter assay

NF- κ B (nuclear factor kappa B) is a key mediator of inflammation and is activated by potent pro-inflammatory cytokines. The results of the NF- κ B reporter assay showed that azithromycin down regulated NF- κ B gene expression induced by LPS. Azithromycin was showed to suppress the activation of NF- κ B and consequently the synthesis of pro-inflammatory cytokines (121, 122).

Cytokine expression after azithromycin stimulation

Azithromycin has been showed to decrease the expression of the pro-inflammatory cytokines IL-1 β and IL-1 α *in vitro* and *in vivo* (69, 123) being a suitable candidate for the treatment of chronic respiratory infections. Our results demonstrated a decrease in the expression of IL-1 β and IL-1 α in primary peritoneal macrophages stimulated with AZM. The cells stimulated with ampicillin showed an increase in the cytokines levels as described by Karlstrom *et al* (93). Neither treatment had a significant affect in the cytokine production when compared to cells stimulated with LPS only.

Nitric Oxide production by stimulated peritoneal macrophages

Down-regulation of iNOS expression was clearly observed in the azithromycin treated macrophages ($p < 0.05$) whereas treatment with ampicillin decreased iNOS production in a non-significant manner. Pro-inflammatory M1 but not anti-inflammatory M2 polarized macrophages exhibit up-regulation of iNOS according to Murphy *et al* (70). This finding confirms our experiments that azithromycin shifts the macrophage phenotype to an M2 phenotype.

These results taken together suggest that azithromycin is stimulating the wound healing of mice periapical lesion by facilitating macrophage polarization to an anti-inflammatory M2 phenotype.

Conclusions

- Azithromycin is a practical approach for shifting the macrophage polarization to an M2 macrophage phenotype *in vitro* and *in vivo*.
- Azithromycin treatment led to immunomodulation of macrophages, an M2-dominant profile from a mixed macrophage profile, in the mice periapical lesion.
- Azithromycin-mediated M2 polarization in the periradicular tissues triggered subsequent wound healing via down regulation of NF- κ B and subsequent production of pro-inflammatory cytokines and iNOS.
- Azithromycin treatment also up-regulated osteogenic genes and might be involved in bone healing, resulting in reduction of periapical lesion size.
- This study suggests the therapeutic potential of immunomodulation targeting M2 macrophages for accelerated healing of apical periodontitis. The dual role of azithromycin, microbicidal and immunomodulatory effects, could pose as a great adjuvant on the root canal therapy being highly translational.

References

1. Kakehashi S, Stanley HR, Fitzgerald RJ. The Effects Of Surgical Exposures Of Dental Pulp In Germ-Free And Conventional Laboratory Rats. *Oral surgery, oral medicine, and oral pathology* 1965;20:340-349.
2. Sundqvist G. Bacteriological studies of necrotic dental pulp. *Umae Univ Odontological Dissertations* 7, 1; 1976.
3. Siqueira JF, Jr., Rocas IN. Diversity of endodontic microbiota revisited. *Journal of dental research* 2009;88(11):969-981.
4. Ozok AR, Persoon IF, Huse SM, Keijser BJ, Wesselink PR, Crielaard W, et al. Ecology of the microbiome of the infected root canal system: a comparison between apical and coronal root segments. *International endodontic journal* 2012;45(6):530-541.
5. Baumgartner JC, Falkler WA, Jr. Bacteria in the apical 5 mm of infected root canals. *Journal of endodontics* 1991;17(8):380-383.
6. Gomes BP, Pinheiro ET, Gade-Neto CR, Sousa EL, Ferraz CC, Zaia AA, et al. Microbiological examination of infected dental root canals. *Oral microbiology and immunology* 2004;19(2):71-76.
7. Moller AJ, Fabricius L, Dahlen G, Ohman AE, Heyden G. Influence on periapical tissues of indigenous oral bacteria and necrotic pulp tissue in monkeys. *Scandinavian journal of dental research* 1981;89(6):475-484.
8. Nair PN. Apical periodontitis: a dynamic encounter between root canal infection and host response. *Periodontology* 2000 1997;13:121-148.
9. Lin L. Pathobiology of the Periapex. In: Cohen S, editor. *Pathways of the Pulp*. St. Louis, Missouri: Mosby Elsevier; 2011. p. 529-558.
10. Sica A, Mantovani A. Macrophage plasticity and polarization: in vivo veritas. *The Journal of clinical investigation* 2012;122(3):787-795.
11. Parnham MJ, Erakovic Haber V, Giamarellos-Bourboulis EJ, Perletti G, Verleden GM, Vos R. Azithromycin: mechanisms of action and their relevance for clinical applications. *Pharmacology & therapeutics* 2014;143(2):225-245.
12. Nair PN, Sjogren U, Figdor D, Sundqvist G. Persistent periapical radiolucencies of root-filled human teeth, failed endodontic treatments, and periapical scars. *Oral surgery, oral medicine, oral pathology, oral radiology, and endodontics* 1999;87(5):617-627.
13. Friedman S, Mor C. The success of endodontic therapy--healing and functionality. *Journal of the California Dental Association* 2004;32(6):493-503.
14. Friedman S, Abitbol S, Lawrence HP. Treatment outcome in endodontics: the Toronto Study. Phase 1: initial treatment. *Journal of endodontics* 2003;29(12):787-793.
15. Sjogren U, Hagglund B, Sundqvist G, Wing K. Factors affecting the long-term results of endodontic treatment. *Journal of endodontics* 1990;16(10):498-504.
16. Sasaki H, Hirai K, Martins CM, Furusho H, Battaglino R, Hashimoto K. Interrelationship between Periapical Lesion and Systemic Metabolic Disorders. *Current pharmaceutical design* 2016.

17. CDC. National Diabetes Fact Sheet. In. Center for Disease Control and Prevention; July 2015.
18. Webb DJ, Colman MF, Thompson K, Wescott WB. Acute, life-threatening disease first appearing as odontogenic pain. *Journal of the American Dental Association* (1939) 1984;109(6):936-938.
19. Robertson D, Smith AJ. The microbiology of the acute dental abscess. *Journal of medical microbiology* 2009;58(Pt 2):155-162.
20. Hsiao WW, Li KL, Liu Z, Jones C, Fraser-Liggett CM, Fouad AF. Microbial transformation from normal oral microbiota to acute endodontic infections. *BMC genomics* 2012;13:345.
21. Nalliah RP, Allareddy V, Elangovan S, Karimbux N, Lee MK, Gajendrareddy P, et al. Hospital emergency department visits attributed to pulpal and periapical disease in the United States in 2006. *Journal of endodontics* 2011;37(1):6-9.
22. Nair PN. Pathogenesis of apical periodontitis and the causes of endodontic failures. *Critical reviews in oral biology and medicine : an official publication of the American Association of Oral Biologists* 2004;15(6):348-381.
23. Graves DT, Oates T, Garlet GP. Review of osteoimmunology and the host response in endodontic and periodontal lesions. *Journal of oral microbiology* 2011;3.
24. Hirao K, Yumoto H, Takahashi K, Mukai K, Nakanishi T, Matsuo T. Roles of TLR2, TLR4, NOD2, and NOD1 in pulp fibroblasts. *Journal of dental research* 2009;88(8):762-767.
25. Hou L, Sasaki H, Stashenko P. Toll-like receptor 4-deficient mice have reduced bone destruction following mixed anaerobic infection. *Infection and immunity* 2000;68(8):4681-4687.
26. Yu SM, Stashenko P. Identification of inflammatory cells in developing rat periapical lesions. *Journal of endodontics* 1987;13(11):535-540.
27. Marton IJ, Kiss C. Characterization of inflammatory cell infiltrate in dental periapical lesions. *International endodontic journal* 1993;26(2):131-136.
28. Stern MH, Dreizen S, Mackler BF, Selbst AG, Levy BM. Quantitative analysis of cellular composition of human periapical granuloma. *Journal of endodontics* 1981;7(3):117-122.
29. Kawashima N, Okiji T, Kosaka T, Suda H. Kinetics of macrophages and lymphoid cells during the development of experimentally induced periapical lesions in rat molars: a quantitative immunohistochemical study. *Journal of endodontics* 1996;22(6):311-316.
30. Stashenko P, Teles R, D'Souza R. Periapical inflammatory responses and their modulation. *Critical reviews in oral biology and medicine : an official publication of the American Association of Oral Biologists* 1998;9(4):498-521.
31. Sasaki H, Hou L, Belani A, Wang CY, Uchiyama T, Muller R, et al. IL-10, but not IL-4, suppresses infection-stimulated bone resorption in vivo. *Journal of immunology (Baltimore, Md. : 1950)* 2000;165(7):3626-3630.
32. Ricucci D, Siqueira JF, Jr., Bate AL, Pitt Ford TR. Histologic investigation of root canal-treated teeth with apical periodontitis: a retrospective study from twenty-four patients. *Journal of endodontics* 2009;35(4):493-502.

33. Nathan C. Metchnikoff's Legacy in 2008. *Nature immunology* 2008;9(7):695-698.
34. Abbas A. Cellular & Molecular Immunology, 7e. In: Abbas A, editor. Philadelphia, PA: Elsevier Saunders; 2012. p. 15-35.
35. Mosser DM, Edwards JP. Exploring the full spectrum of macrophage activation. *Nature reviews. Immunology* 2008;8(12):958-969.
36. Hato T, Dagher PC. How the Innate Immune System Senses Trouble and Causes Trouble. *Clinical journal of the American Society of Nephrology : CJASN* 2015;10(8):1459-1469.
37. Zhou L, Cao X, Fang J, Li Y, Fan M. Macrophages polarization is mediated by the combination of PRR ligands and distinct inflammatory cytokines. *International journal of clinical and experimental pathology* 2015;8(9):10964-10974.
38. Anders HJ, Ryu M. Renal microenvironments and macrophage phenotypes determine progression or resolution of renal inflammation and fibrosis. *Kidney international* 2011;80(9):915-925.
39. Kadl A, Meher AK, Sharma PR, Lee MY, Doran AC, Johnstone SR, et al. Identification of a novel macrophage phenotype that develops in response to atherogenic phospholipids via Nrf2. *Circulation research* 2010;107(6):737-746.
40. Gordon S, Taylor PR. Monocyte and macrophage heterogeneity. *Nature reviews. Immunology* 2005;5(12):953-964.
41. Edwards JP, Zhang X, Frauwirth KA, Mosser DM. Biochemical and functional characterization of three activated macrophage populations. *Journal of leukocyte biology* 2006;80(6):1298-1307.
42. Mantovani A, Sica A, Sozzani S, Allavena P, Vecchi A, Locati M. The chemokine system in diverse forms of macrophage activation and polarization. *Trends in immunology* 2004;25(12):677-686.
43. Sima C, Glogauer M. Macrophage subsets and osteoimmunology: tuning of the immunological recognition and effector systems that maintain alveolar bone. *Periodontology 2000* 2013;63(1):80-101.
44. Biswas SK, Mantovani A. Macrophage plasticity and interaction with lymphocyte subsets: cancer as a paradigm. *Nature immunology* 2010;11(10):889-896.
45. Genin M, Clement F, Fattaccioli A, Raes M, Michiels C. M1 and M2 macrophages derived from THP-1 cells differentially modulate the response of cancer cells to etoposide. *BMC cancer* 2015;15:577.
46. Morris SM, Jr., Kepka-Lenhart D, Chen LC. Differential regulation of arginases and inducible nitric oxide synthase in murine macrophage cells. *The American journal of physiology* 1998;275(5 Pt 1):E740-747.
47. Rath M, Muller I, Kropf P, Closs EI, Munder M. Metabolism via Arginase or Nitric Oxide Synthase: Two Competing Arginine Pathways in Macrophages. *Frontiers in immunology* 2014;5:532.
48. Gould A NC, Candy GP. Arginine metabolism and wound healing. *Wound Healing Southern Africa* 2008;1(1):48-50.
49. Davis MJ, Tsang TM, Qiu Y, Dayrit JK, Freij JB, Huffnagle GB, et al. Macrophage M1/M2 polarization dynamically adapts to changes in cytokine microenvironments in *Cryptococcus neoformans* infection. *mBio* 2013;4(3):e00264-00213.

50. Laskin DL, Sunil VR, Gardner CR, Laskin JD. Macrophages and tissue injury: agents of defense or destruction? *Annual review of pharmacology and toxicology* 2011;51:267-288.
51. Roland CR, Mangino MJ, Duffy BF, Flye MW. Lymphocyte suppression by Kupffer cells prevents portal venous tolerance induction: a study of macrophage function after intravenous gadolinium. *Transplantation* 1993;55(5):1151-1158.
52. Lazar G. The reticuloendothelial-blocking effect of rare earth metals in rats. *Journal of the Reticuloendothelial Society* 1973;13(3):231-237.
53. Yang XC, Sachs F. Block of stretch-activated ion channels in *Xenopus* oocytes by gadolinium and calcium ions. *Science (New York, N.Y.)* 1989;243(4894 Pt 1):1068-1071.
54. Boland LM, Brown TA, Dingle R. Gadolinium block of calcium channels: influence of bicarbonate. *Brain research* 1991;563(1-2):142-150.
55. Adding LC, Bannenberg GL, Gustafsson LE. Basic experimental studies and clinical aspects of gadolinium salts and chelates. *Cardiovascular drug reviews* 2001;19(1):41-56.
56. Miron VE, Boyd A, Zhao JW, Yuen TJ, Ruckh JM, Shadrach JL, et al. M2 microglia and macrophages drive oligodendrocyte differentiation during CNS remyelination. *Nature neuroscience* 2013;16(9):1211-1218.
57. Pendino KJ, Meidhof TM, Heck DE, Laskin JD, Laskin DL. Inhibition of macrophages with gadolinium chloride abrogates ozone-induced pulmonary injury and inflammatory mediator production. *American journal of respiratory cell and molecular biology* 1995;13(2):125-132.
58. Van Rooijen N, Sanders A. Kupffer cell depletion by liposome-delivered drugs: comparative activity of intracellular clodronate, propamide, and ethylenediaminetetraacetic acid. *Hepatology (Baltimore, Md.)* 1996;23(5):1239-1243.
59. Mazzei T, Mini E, Novelli A, Periti P. Chemistry and mode of action of macrolides. *The Journal of antimicrobial chemotherapy* 1993;31 Suppl C:1-9.
60. Williams JD, Sefton AM. Comparison of macrolide antibiotics. *The Journal of antimicrobial chemotherapy* 1993;31 Suppl C:11-26.
61. Zhanel GG, Dueck M, Hoban DJ, Vercaigne LM, Embil JM, Gin AS, et al. Review of macrolides and ketolides: focus on respiratory tract infections. *Drugs* 2001;61(4):443-498.
62. Champney WS, Burdine R. Azithromycin and clarithromycin inhibition of 50S ribosomal subunit formation in *Staphylococcus aureus* cells. *Current microbiology* 1998;36(2):119-123.
63. Hoffmann N, Lee B, Hentzer M, Rasmussen TB, Song Z, Johansen HK, et al. Azithromycin blocks quorum sensing and alginate polymer formation and increases the sensitivity to serum and stationary-growth-phase killing of *Pseudomonas aeruginosa* and attenuates chronic *P. aeruginosa* lung infection in *Cftr(-/-)* mice. *Antimicrobial agents and chemotherapy* 2007;51(10):3677-3687.
64. Amsden GW. Advanced-generation macrolides: tissue-directed antibiotics. *International journal of antimicrobial agents* 2001;18 Suppl 1:S11-15.

65. Lode H, Borner K, Koeppe P, Schaberg T. Azithromycin--review of key chemical, pharmacokinetic and microbiological features. *The Journal of antimicrobial chemotherapy* 1996;37 Suppl C:1-8.
66. Foulds G, Shepard RM, Johnson RB. The pharmacokinetics of azithromycin in human serum and tissues. *The Journal of antimicrobial chemotherapy* 1990;25 Suppl A:73-82.
67. Gomi K, Yashima A, Iino F, Kanazashi M, Nagano T, Shibukawa N, et al. Drug concentration in inflamed periodontal tissues after systemically administered azithromycin. *Journal of periodontology* 2007;78(5):918-923.
68. Culic O, Erakovic V, Cepelak I, Barisic K, Brajsa K, Ferencic Z, et al. Azithromycin modulates neutrophil function and circulating inflammatory mediators in healthy human subjects. *European journal of pharmacology* 2002;450(3):277-289.
69. Khan AA, Slifer TR, Araujo FG, Remington JS. Effect of clarithromycin and azithromycin on production of cytokines by human monocytes. *International journal of antimicrobial agents* 1999;11(2):121-132.
70. Murphy BS, Sundareshan V, Cory TJ, Hayes D, Jr., Anstead MI, Feola DJ. Azithromycin alters macrophage phenotype. *The Journal of antimicrobial chemotherapy* 2008;61(3):554-560.
71. Feola DJ, Garvy BA, Cory TJ, Birket SE, Hoy H, Hayes D, Jr., et al. Azithromycin alters macrophage phenotype and pulmonary compartmentalization during lung infection with *Pseudomonas*. *Antimicrobial agents and chemotherapy* 2010;54(6):2437-2447.
72. Hodge S, Hodge G, Jersmann H, Matthews G, Ahern J, Holmes M, et al. Azithromycin improves macrophage phagocytic function and expression of mannose receptor in chronic obstructive pulmonary disease. *American journal of respiratory and critical care medicine* 2008;178(2):139-148.
73. Amantea D, Certo M, Petrelli F, Tassorelli C, Micieli G, Corasaniti MT, et al. Azithromycin protects mice against ischemic stroke injury by promoting macrophage transition towards M2 phenotype. *Experimental neurology* 2016;275 Pt 1:116-125.
74. MacLeod AS, Mansbridge JN. The Innate Immune System in Acute and Chronic Wounds. *Advances in wound care* 2016;5(2):65-78.
75. Koh TJ, DiPietro LA. Inflammation and wound healing: the role of the macrophage. *Expert reviews in molecular medicine* 2011;13:e23.
76. Brown BN, Ratner BD, Goodman SB, Amar S, Badylak SF. Macrophage polarization: an opportunity for improved outcomes in biomaterials and regenerative medicine. *Biomaterials* 2012;33(15):3792-3802.
77. Trudel L, St-Amand L, Bareil M, Cardinal P, Lavoie MC. Bacteriology of the oral cavity of BALB/c mice. *Canadian journal of microbiology* 1986;32(8):673-678.
78. Fraser CC, Chen BP, Webb S, van Rooijen N, Kraal G. Circulation of human hematopoietic cells in severe combined immunodeficient mice after Cl2MDP-liposome-mediated macrophage depletion. *Blood* 1995;86(1):183-192.
79. Balto K, Muller R, Carrington DC, Dobeck J, Stashenko P. Quantification of periapical bone destruction in mice by micro-computed tomography. *Journal of dental research* 2000;79(1):35-40.

80. Smale ST. Luciferase assay. Cold Spring Harbor protocols 2010;2010(5):pdb prot5421.
81. Metzger Z. Macrophages in periapical lesions. Endodontics & dental traumatology 2000;16(1):1-8.
82. Saiman L, Marshall BC, Mayer-Hamblett N, Burns JL, Quittner AL, Cibene DA, et al. Azithromycin in patients with cystic fibrosis chronically infected with *Pseudomonas aeruginosa*: a randomized controlled trial. *Jama* 2003;290(13):1749-1756.
83. Equi A, Balfour-Lynn IM, Bush A, Rosenthal M. Long term azithromycin in children with cystic fibrosis: a randomised, placebo-controlled crossover trial. *Lancet (London, England)* 2002;360(9338):978-984.
84. Liapatas S, Nakou M, Rontogianni D. Inflammatory infiltrate of chronic periradicular lesions: an immunohistochemical study. *International endodontic journal* 2003;36(7):464-471.
85. Ricucci D, Mannocci F, Ford TR. A study of periapical lesions correlating the presence of a radiopaque lamina with histological findings. *Oral surgery, oral medicine, oral pathology, oral radiology, and endodontics* 2006;101(3):389-394.
86. Garcia CC, Sempere FV, Diago MP, Bowen EM. The post-endodontic periapical lesion: histologic and etiopathogenic aspects. *Medicina oral, patologia oral y cirugia bucal* 2007;12(8):E585-590.
87. Wang CY, Stashenko P. The role of interleukin-1 alpha in the pathogenesis of periapical bone destruction in a rat model system. *Oral microbiology and immunology* 1993;8(1):50-56.
88. Kawashima N, Stashenko P. Expression of bone-resorptive and regulatory cytokines in murine periapical inflammation. *Archives of oral biology* 1999;44(1):55-66.
89. Han DC, Huang GT, Lin LM, Warner NA, Gim JS, Jewett A. Expression of MHC Class II, CD70, CD80, CD86 and pro-inflammatory cytokines is differentially regulated in oral epithelial cells following bacterial challenge. *Oral microbiology and immunology* 2003;18(6):350-358.
90. Wang P, Wu P, Siegel MI, Egan RW, Billah MM. Interleukin (IL)-10 inhibits nuclear factor kappa B (NF kappa B) activation in human monocytes. IL-10 and IL-4 suppress cytokine synthesis by different mechanisms. *The Journal of biological chemistry* 1995;270(16):9558-9563.
91. Porta C, Riboldi E, Ippolito A, Sica A. Molecular and epigenetic basis of macrophage polarized activation. *Seminars in immunology* 2015;27(4):237-248.
92. Pagliari LJ, Perlman H, Liu H, Pope RM. Macrophages require constitutive NF-kappaB activation to maintain A1 expression and mitochondrial homeostasis. *Molecular and cellular biology* 2000;20(23):8855-8865.
93. Karlstrom A, Boyd KL, English BK, McCullers JA. Treatment with protein synthesis inhibitors improves outcomes of secondary bacterial pneumonia after influenza. *The Journal of infectious diseases* 2009;199(3):311-319.
94. Gao X, Ray R, Xiao Y, Ray P. Suppression of inducible nitric oxide synthase expression and nitric oxide production by macrolide antibiotics in sulfur mustard-exposed airway epithelial cells. *Basic & clinical pharmacology & toxicology* 2008;103(3):255-261.

95. Fouad A, Barry J, Russo J, Radolf J, Zhu Q. Periapical lesion progression with controlled microbial inoculation in a type I diabetic mouse model. *Journal of endodontics* 2002;28(1):8-16.
96. Stein M, Keshav S, Harris N, Gordon S. Interleukin 4 potently enhances murine macrophage mannose receptor activity: a marker of alternative immunologic macrophage activation. *The Journal of experimental medicine* 1992;176(1):287-292.
97. Brown M, Wittwer C. Flow cytometry: principles and clinical applications in hematology. *Clinical chemistry* 2000;46(8 Pt 2):1221-1229.
98. Hardonk MJ, Dijkhuis FW, Hulstaert CE, Koudstaal J. Heterogeneity of rat liver and spleen macrophages in gadolinium chloride-induced elimination and repopulation. *Journal of leukocyte biology* 1992;52(3):296-302.
99. Van Rooijen N, Sanders A. Liposome mediated depletion of macrophages: mechanism of action, preparation of liposomes and applications. *Journal of immunological methods* 1994;174(1-2):83-93.
100. Dave J, Patel HM. Differentiation in hepatic and splenic phagocytic activity during reticuloendothelial blockade with cholesterol-free and cholesterol-rich liposomes. *Biochimica et biophysica acta* 1986;888(2):184-190.
101. Zhang B, Bailey WM, Kopper TJ, Orr MB, Feola DJ, Gensel JC. Azithromycin drives alternative macrophage activation and improves recovery and tissue sparing in contusion spinal cord injury. *Journal of neuroinflammation* 2015;12:218.
102. Piacentini GL, Peroni DG, Bodini A, Pigozzi R, Costella S, Loiacono A, et al. Azithromycin reduces bronchial hyperresponsiveness and neutrophilic airway inflammation in asthmatic children: a preliminary report. *Allergy and asthma proceedings : the official journal of regional and state allergy societies* 2007;28(2):194-198.
103. Blasi F, Bonardi D, Aliberti S, Tarsia P, Confalonieri M, Amir O, et al. Long-term azithromycin use in patients with chronic obstructive pulmonary disease and tracheostomy. *Pulmonary pharmacology & therapeutics* 2010;23(3):200-207.
104. Basyigit I, Yildiz F, Ozkara SK, Yildirim E, Boyaci H, Ilgazli A. The effect of clarithromycin on inflammatory markers in chronic obstructive pulmonary disease: preliminary data. *The Annals of pharmacotherapy* 2004;38(9):1400-1405.
105. Lu G, Zhang R, Geng S, Peng L, Jayaraman P, Chen C, et al. Myeloid cell-derived inducible nitric oxide synthase suppresses M1 macrophage polarization. *Nature communications* 2015;6:6676.
106. Martinez FO, Helming L, Gordon S. Alternative activation of macrophages: an immunologic functional perspective. *Annual review of immunology* 2009;27:451-483.
107. Bogdan C. Nitric oxide and the immune response. *Nature immunology* 2001;2(10):907-916.
108. Graunaite I, Lodiene G, Maciulskiene V. Pathogenesis of apical periodontitis: a literature review. *Journal of oral & maxillofacial research* 2012;2(4):e1.
109. Lin SK, Kok SH, Lin LD, Wang CC, Kuo MY, Lin CT, et al. Nitric oxide promotes the progression of periapical lesion via inducing macrophage and osteoblast apoptosis. *Oral microbiology and immunology* 2007;22(1):24-29.

110. Gyurko R, Shoji H, Battaglino RA, Boustany G, Gibson FC, 3rd, Genco CA, et al. Inducible nitric oxide synthase mediates bone development and P. gingivalis-induced alveolar bone loss. *Bone* 2005;36(3):472-479.
111. Barkhordar RA, Hayashi C, Hussain MZ. Detection of interleukin-6 in human dental pulp and periapical lesions. *Endodontics & dental traumatology* 1999;15(1):26-27.
112. de Sa AR, Moreira PR, Xavier GM, Sampaio I, Kalapothakis E, Dutra WO, et al. Association of CD14, IL1B, IL6, IL10 and TNFA functional gene polymorphisms with symptomatic dental abscesses. *International endodontic journal* 2007;40(7):563-572.
113. Radics T, Kiss C, Tar I, Marton IJ. Interleukin-6 and granulocyte-macrophage colony-stimulating factor in apical periodontitis: correlation with clinical and histologic findings of the involved teeth. *Oral microbiology and immunology* 2003;18(1):9-13.
114. Ishimi Y, Miyaura C, Jin CH, Akatsu T, Abe E, Nakamura Y, et al. IL-6 is produced by osteoblasts and induces bone resorption. *Journal of immunology (Baltimore, Md. : 1950)* 1990;145(10):3297-3303.
115. Huang GT, Do M, Wingard M, Park JS, Chugal N. Effect of interleukin-6 deficiency on the formation of periapical lesions after pulp exposure in mice. *Oral surgery, oral medicine, oral pathology, oral radiology, and endodontics* 2001;92(1):83-88.
116. Balto K, Sasaki H, Stashenko P. Interleukin-6 deficiency increases inflammatory bone destruction. *Infection and immunity* 2001;69(2):744-750.
117. Hart PH, Vitti GF, Burgess DR, Whitty GA, Piccoli DS, Hamilton JA. Potential antiinflammatory effects of interleukin 4: suppression of human monocyte tumor necrosis factor alpha, interleukin 1, and prostaglandin E2. *Proceedings of the National Academy of Sciences of the United States of America* 1989;86(10):3803-3807.
118. Maeda H, Wada N, Nakamuta H, Akamine A. Human periapical granulation tissue contains osteogenic cells. *Cell and tissue research* 2004;315(2):203-208.
119. Rittling SR, Zetterberg C, Yagiz K, Skinner S, Suzuki N, Fujimura A, et al. Protective role of osteopontin in endodontic infection. *Immunology* 2010;129(1):105-114.
120. Zhang X, Peng B. Immunolocalization of receptor activator of NF kappa B ligand in rat periapical lesions. *Journal of endodontics* 2005;31(8):574-577.
121. Aghai ZH, Kode A, Saslow JG, Nakhla T, Farhath S, Stahl GE, et al. Azithromycin suppresses activation of nuclear factor-kappa B and synthesis of pro-inflammatory cytokines in tracheal aspirate cells from premature infants. *Pediatric research* 2007;62(4):483-488.
122. Cheung PS, Si EC, Hosseini K. Anti-inflammatory activity of azithromycin as measured by its NF-kappaB, inhibitory activity. *Ocular immunology and inflammation* 2010;18(1):32-37.
123. Majima Y. Clinical implications of the immunomodulatory effects of macrolides on sinusitis. *The American journal of medicine* 2004;117 Suppl 9A:20S-25S.

